# Grape exosome-like nanoparticles, a novel inducer of intestinal stem cells, protect mice against DSS induced colitis

Songwen Ju, Jingyao Mu, Terje Dokland, Xiaoying Zhuang, Qilong Wang, Hong Jiang, Xiaoyu Xiang, Zhong-Bin Deng, Baomei Wang, Lifeng Zhang, Mary Roth, Ruth Welti, James Mobley, Yan Jun, Donald Miller, and Huang-Ge Zhang



**Published Version Information**

**Citation**: Ju, S., Mu, J., Dokland, T., Zhuang, X., Wang, Q., Jiang, H., . . . Zhang, H.-G. (2013). Grape exosome-like nanoparticles induce intestinal stem cells and protect mice from DSS-induced colitis. Molecular Therapy, 21(7), 1345-1357.



**Digital Object Identifier (DOI)**: doi:10.1038/mt.2013.64

**Publisher's Link**: http://www.nature.com/mt/journal/v21/n7/full/mt201364a.html

# Grape exosome-like nanoparticles, a novel inducer of intestinal stem cells, protect mice against DSS induced colitis

Songwen Ju[2], Jingyao Mu[2], Terje Dokland[3], Xiaoying Zhuang[2], Qilong Wang[2], Hong Jiang[2], Xiaoyu Xiang[2], Zhong-Bin Deng[2], Baomei Wang[2], Lifeng Zhang[2], Mary Roth[5], Ruth Welti[5], James Mobley[4], Yan Jun[2], Donald Miller[2], and Huang-Ge Zhang[1, 2,*]

[1]Louisville Veterans Administration Medical Center, Louisville, KY40206
[2]Brown Cancer Center, Department of Microbiology & Immunology, University of Louisville, KY40202
[3]Department of Microbiology, University of Alabama at Birmingham, Birmingham, AL35294
[4]Department of Radiology, University of Alabama at Birmingham, Birmingham, AL35294
[5]Kansas Lipidomics Research Center, Division of Biology, Kansas State University, Manhattan, KS66506

[*] Address correspondence and reprint requests to:
Dr. Huang-Ge Zhang
Brown Cancer Center
University of Louisville
CTRB 309
505 Hancock Street
Louisville, KY40202
E-mail address: H0Zhan17@louisville.edu

Songwen Ju, and Jingyao Mu contributed equally to this work.

A running title: Induction of stem cells by edible nanoparticles

Key words: Grape exosome-like nanoparticles; exosomes; lipids; intestinal stem cell; Wnt/β-catenin pathway

Abstract

Food derived exosome-like nanoparticles pass through the intestinal tract throughout our lives, but little is known about their impact or function. Here, as a proof of concept, we show that the cells targeted by grape exosome-like nanoparticles (GELNs) are intestinal stem cells whose responses underlie the GELN-mediated intestinal tissue remodeling and protection against dextran sulfate sodium (DSS) induced colitis. This finding is further supported by the fact that co-culturing of crypt or sorted $Lgr5^+$ stem cells with GELNs markedly improved organoid formation. GELN lipids play a role in induction of $Lgr5^+$ stem cells, and the liposome-like nanoparticles (LLNs) assembled with lipids from GELNs are required for in vivo targeting of intestinal stem cells. Blocking β-catenin mediated signaling pathways of GELN recipient cells attenuates the production of $Lgr5^+$ stem cells. Thus, GELNs not only modulate intestinal tissue renewal processes, but can participate in the remodeling of it in response to pathological triggers.

## Introduction

In multicellular organisms communication between cells involves the secretion of proteins that bind to receptors on neighboring cells. While this is well documented, another mode of intercellular communication — the release of exosomes, for which limited information is known — has recently become a subject of increasing interest. Exosomes are nano-sized microvesicles released from a variety of cells[1-6] and have recently been described to act on the endocrine system to provide autocrine or paracrine signals locally or at distant sites in the host. Exosomes can carry a cargo of

proteins, lipids, mRNAs and/or microRNAs, and can transfer their cargo to recipient cells, thus serving as extracellular messengers to mediate cell-cell communication.

Recent studies suggest that nano-sized particles from plant cells may be exosome-like[7, 8]. Endosomal multivesicular body (MVB)-derived exosome-like nanoparticles in plant cells may be involved in plant cell-cell communication as a means to regulate plant innate immunity[9]. Plant viruses may hijack the exosomal pathway of a plant as a way to release virus[10]. However, whether plant exosome-like nanoparticles can play a role in interspecies communication has not been investigated, yet, human exposure to digested edible plant derived nano-size materials is inevitable. The average person's gut is exposed on a daily basis to many billions of nanoparticles. The gastrointestinal tract may communicate directly with the external environment through digested food including edible plant derived exosome-like nanoparticles. Whether these edible plant-derived exosome-like nanoparticles can serve as cross-species messengers and have a biological effect on the recipient cells in the intestinal tract has not been addressed. More specifically, little is known about the biological effects of exosome-like nanoparticles released from edible plants on intestinal tissue remodeling after oral ingestion of the nanoparticles.

In this study, exosome-like nanoparticles were identified from grapes. Using grape exosome-like nanoparticles (GELNs) as proof of concept testing, we demonstrate that GELNs have unique transport properties and biological functions. GELNs can penetrate the intestinal mucus barrier, be taken up by mouse intestinal stem cells and cause significant induction of $Lgr5^{hi}$ intestinal stem cells through the Wnt/β-catenin pathway.

Oral administration of GELNs leads to protection of mice from DSS induced colitis via induction of intestinal stem cells. This finding could lead to the development of novel, safe, and economical strategies for using edible plant derived nanoparticles as nano-size therapeutic agents or as an alternative drug delivery vehicle, as well as opening up a new avenue for food nanotechnology.

## Results

### Intestinal stem cells take up grape exosome-like nanoparticles

Using standard techniques [11], we isolated edible plant exosome-like nanoparticles from the juice of grapes. The particles were identifiable as exosome-like nanoparticles based on electron microscopy examination (Figure 1a, right) of a sucrose gradient purified band (Figure 1a, left), charge, size distribution (Figure 1b), protein composition (Supplementary table S1), lipid profile (Supplementary table S2) and the miRNA profile (Supplementary Table S3). The results indicated that the particles are nano-size and the average diameter of the particle population was 380.5 ± 37.47 nm (Fig. 1*b*). Zeta potential measurements indicated that GELNs have a negative zeta potential value ranging from -69.6 mV to +2.52 mV and the average potential of the particle population was -26.3 ± 8.14 mV (Fig. 1*b*).

Lipidomic data indicate that GELNs are enriched with PA (53.2%) and PE (26.1%) (Figure 1c). Unusually high percentages of PA in GELNs could result from activation of GELN phospholipase D, (PLD) during the process of extraction of GELN lipids. However, this was not the case as indicated by lipidomic analysis of lipids extracted from either whole grape or GELNs in the presence or absence of 75% isopropanol in

PBS at 75°C during the extraction of lipids [12, 13]. The percentage of GELN PA remains the same in the presence (47.2±5.2%, n=5) versus absence (49.1±3.8%m n=5) of 75% isopropanol. Interestingly, the percentage of PA in whole grape is much lower (18.2±1.9%) than its GELN (47.2±5.2%) counterpart extracted from the same lot of grapes. This result suggests that higher amounts of PA present in GELNs could be due to selectively sorting PA into the GELNs. The presence of nucleic acids was also examined in GELNs. Substantial amounts of RNAs were detected by agarose gel electrophoresis. RNase treatment lead to the degradation of GELN RNA samples (Figure 1d). Mass spectrometry analysis of the GELN miRNA profile further suggested that GELNs contain miRNAs (Supplemental table 3). Collectively, these data demonstrated that our preparation contained a high proportion of grape-derived exosome-like nanoparticles.

Intestinal mucus is a physically cross-linked hydrogel[14-17]. Penetration of this barrier is largely dependent on the size of the particles[14-17]. A majority of grape derived exosome-like nanoparticles is nanosized and we used gavage administration of GELNs labeled with an infrared fluorescent membrane dye (DiR) to track their migration patterns *in vivo*[18]. Imaging revealed an accumulation of fluorescent signals in the gut during the first 6 h (Fig. 2a), then the signals gradually decreased over a 48 h period (Fig. 2a). The presence of GELNs in stem cells of the intestine of Lgr5-EGFP-IRES-CreERT2 mice was confirmed by localization of PKH26-labeled GELNs to the Lgr5-EGFP$^{+}$ marker, a marker of intestinal stem cells (Fig. 2b). Within 6 h of administration of the labeled GELNs, the GELNs were taken up by intestinal Lgr5-EGFP$^{+}$ stem cells.

Thus, GELNs can gain access to, and travel within the gut to the intestinal stem cells. The uptake of PKH26-labeled GELNs was further examined using the mouse intestinal epithelial cell line CT26. Three h after CT26 cells were fed with PKH26-labeled GELNs, most of the CT26 cells had PKH26-labeled GELNs located in the cytosol (Figure 2c). The uptake mechanism of PKH26-labeled GELNs was further examined in the CT26 cell line. Uptake of GELNs (Figure 2d) was markedly inhibited by the cytochalasin D, known as a macropinocytosis inhibitor. Uptake of GELNs through macropinocytosis was also demonstrated by cytochalasin D mediated inhibition of uptake of both GELNs as well as dextran (Supplemental figure 1) which is one of fluid phase markers for studying macropinocytosis. In addition, uptake of PKH26-GELNs was greatly diminished by treatment of CT26 cells with the macrolide antibiotics bafilomycin A1 and concanamycin A, which are highly specific V-ATPase inhibitors [19] that prevent proton translocation by binding to the c-subunit of the V-ATPase $V_0$ subunit[20]. Caveolae-mediated endocytosis inhibitor indomethacin and the clathrin-mediated endocytosis inhibitor chlorpromazine did not affect uptake of PKH26-GELNs. To further confirm whether the same pathway of CT26 cells uptake of GELNs was also used in vivo, the colon tissues of Lgr5-EGFP-IRES-CreERT2 mice were ex vivo co-cultured with PKH26 dye labeled GELNs in the presence/absence of the cytochalasin D. The results suggest that the cytochalasin D treatment indeed inhibited GELNs up take by colon intestinal stem cells (Fig. 2e).

**GELNs promote intestinal stem cell proliferation**

Self-renewal of the intestinal epithelium is essential for protection of the host against numerous insults. Self-renewal is driven by the proliferation of stem cells and their progenitors located in the intestinal crypts. To explore the biological effects of oral administration of GELNs on intestinal stem cells, we tested the effects of purified GELN treatment of mice on the proliferation of intestinal epithelium. The number of proliferating cells ($Ki67^+$) in intestinal epithelium of mice treated with GELNs was increased when compared to vehicle (PBS) only treated mice. Among the $Ki67^+$ cell population, the Lgr5-$EGFP^+Ki67^+$ cells that are intestinal stem cells were markedly increased (Fig. 3a, 3b). The induction of Lgr5-$EGFP^+Ki67^+$ cells was not restricted to the small intestine but was observed throughout the entire intestine including the colon of mice gavaged with GELNs. The administration of GELNs increased production of intestinal stem cells, as assessed by FACS staining of Lgr5-EGFP cells (Fig. 3b) and quantitative analysis of gene expression of Lgr5 of C57BL/6j mice orally administered with GELNs by real-time PCR (Fig 3c). It has been reported that only the Lgr5-$GFP^{hi}$ cells yield long-lived intestinal organoid structures[21]. Using FACS analysis we identified the presence of two different Lgr5-expressing populations based on GFP levels (Fig. 3b): Lgr5-$EGFP^{hi}$ and Lgr5-$EGFP^{lo}$. GELN treatment induced both subset populations of $EGFP^+$ cells, and especially, the Lgr5-$EGFP^{hi}$ subset was induced more than the Lgr5$EGFP^{lo}$ subset (Fig. 3b). Our *in vivo* data were further verified using 3D matrigel cultures of intestinal crypts from Lgr5-EGFP-IRES-CreERT2 mice. Addition of GELNs to crypt cultures yielded much faster expanding cystic structures within 6 d (Fig. 3d) based on gross inspection. Faster expanding cystic structures was supported by the results generated from a $^3$H-thymidine incorporation assay (Supplemental Fig. 2).

FACS analysis of cells dissociated from day-6 cultured crypts further indicated that the intestinal crypts treated with GELNs had a higher percentage of Lgr5-EGFP$^{hi}$ stem cells induced at extended time points during culture (Fig. 3e) in a GELN dose dependent manner.

To further test whether GELNs can directly induce intestinal stem cells, we isolated Lgr5-EGFP$^{hi}$ stem cells from crypts of Lgr5-EGFP-IRES-CreERT2 mice and subsequently cultured them *in vitro* in the presence of GELNs (40 μg/ml). The results confirmed that the GELNs directly promote the proliferation of Lgr5-EGFP$^{hi}$ intestinal stem cells, and accelerate organoid structure formation (Fig. 3f). Consistent with this, higher efficiency of colony formation as a result of GELNs treatment (Supplemental fig. 3) also support that GELNs stimulate organoid formation.

To further determine whether the liposome-like nanoparticles (LLNs) assembled with lipids from GELNs are required for GELN up take by intestinal Lgr5$^{+}$ stem cells, Lgr5-EGFP-IRES-CreERT2 mice were orally administered PKH26-labeled LLNs (Figure 4a) assembled from GELN derived lipids. Mice were killed 6 h after oral administration and frozen sections of their intestine tissue were examined using confocal microscopy for the presence of the PKH26-labeled LLNs assembled with lipids from GELNs. Fluorescent labeled PKH26-labeled LLNs were observed in Lgr5-EGFP$^{+}$ cells (Figure 4b). In contrast, very little or no fluorescence was detected in the intestine of mice orally administered mixed lipids extracted from GELNs without the assembling process

(Figure 4b). These results suggest that LLNs assembled with GELN lipids are required for targeting intestinal stem cells as well as the cells around Lgr5-EGFP$^{+}$ cells.

We next tested in a defined three-dimensional intestinal culture system whether LLNs assembled with GELN lipids induce Lgr5$^{+}$ stem cells. Flow cytometry analysis of cells dissociated from 6-day cultured crypts demonstrated that Lgr5-EGFP$^{hi+}$ cell numbers increased as the concentration of LLNs assembled with lipids from GELNs was increased (Fig. 4c). Real-time PCR analysis of the expression of the known genes that promote intestinal stem cell growth indicated selective upregulation of Sox2, Nanog, OCT4, KLF4, c-Myc and EGFR in the 6-day cultured crypts (Figure 4d). Similar results were also obtained with the CT26 intestinal epithelial cell line (Supplemental fig.4).

PA is enriched in GELNs, and propranolol has been reported to inhibit the activity of PA-phosphatase[22, 23]. Therefore, we tested whether propranolol treatment of GELNs can effect GELNs induction of Ki67$^{+}$ cells in colon tissue. The results from ex vivo colon tissue culture treated with GELNs which were pre-treated with propranolol suggest that propranolol treatment did lead to decreasing the percentage of Ki67$^{+}$ cells in colon tissue in a propranolol concentration dependent manner (Figure 4e).

**A number of genes that regulate intestinal stem cell growth are induced through the Wnt/β-catenin signaling pathway in the intestine of mice treated with GELNs**

Throughout life, the *Wnt* signal is required for intestinal stem cell self-renewal [24-29]. Analysis of the intestines from canonical Wnt reporter mice, i.e., B6.Cg-Tg(BAT-

lacZ)3Picc/J mice, revealed that the number of expressed β-galactosidase$^{+}$ (β-Gal) intestinal crypts is increased (Figure 5a), suggesting that GELN treatment of mice leads to Wnt mediated activation of the Tcf4 transcription machinery in the crypts. We did real-time PCR assays to analyze gene expression in FACS sorted EGFP$^{hi}$ cells from crypts of Lgr5-EGFP-IRES-CreERT2 mice that had been treated with GELNs or vehicle (PBS). Results showed that the *Wnt* pathway regulated genes, including, AXIN-2, Cyclin D1, c-Myc, and EGFR, were significantly up regulated in Lgr5-EGFP$^{+}$ stem cells (Figure 5b); whereas, expression of Pten[30] and VEGF[31], which have been reported to regulate the proliferation of stem cells, were not affected as a result of GLEN treatment.

Nuclear accumulation of β-catenin is considered a hallmark of activated Tcf4 mediated canonical Wnt signaling. To further confirm that the Tcf4 activity changes were due to activation of β-catenin mediated Wnt activation as a result of GELN treatment, we performed immunofluorescent staining of β-catenin in the CT26 intestinal epithelial cell line treated with GELNs or PBS as a control. The immunofluorescent images clearly showed dramatic nuclear migration of β-catenin in cells 6 h after stimulation with GELNs (Figure 5c, left panel). Activation of the β-catenin mediated pathway was further confirmed by treatment of CT26 with carnosic acid, a β-catenin inhibitor[32] (Figure 5c, right panel), or inactivation of GSK-3β as indicated by an enhancement of phosphorylation of GSK-3β over 180 min as assayed by western blotting (Figure 5d).

Next, to further prove that β-catenin is involved in induction of Lgr5-EGFP$^{+}$ cells, we added carnosic acid to 3D matrigel cultures of intestinal crypts from Lgr5-EGFP-IRES-CreERT2 mice using an identical protocol as described in figure 3f. Flow cytometry analysis of cells dissociated from 6-day cultured crypts demonstrated that GELNs plus carnosic acid treatment leads to a partial reversing of GELN mediated induction of Lgr5-EGFP$^{hi}$ cells (5.1±1.1% carnosic acid plus GELN treated culture versus 8.7±2.3% GELN treated only) (Figure 5e). The results suggest that the addition of β-catenin inhibitor reversed GELN dependent induction of Lgr5-EGFP$^{hi}$ stem cells. Collectively, these data indicate that oral administration of GELNs leads to an induction of genes that encode intestinal stem cell growth factors partially through the Wnt/β-catenin signaling pathway that result in the induction of Lgr5-EGFP$^{hi}$ intestinal stem cells. We also did real-time PCR assays to analyze gene expression in matrigel cultured intestinal crypts of C57BL/6 mice that had been treated with GELNs or vehicle (PBS). Besides the *Wnt* pathway regulated genes, BMI1 another intestinal stem cell marker, and a number of pluripotent stem cell markers, including SOX2, Nanog, OCT4, and KLF4, were also significantly up regulated (Figure 5f)[21, 25, 29, 33-37] .

We then determined whether the LLNs assembled with GELN lipids have a similar activating effect on the Wnt/Tcf4 signaling pathway as GELNs. Using the same protocol as was used for analysis of the effect of GELNs, B6.Cg-Tg(BAT-lacZ)3Picc/J mice were gavage administered daily for 2 days the LLNs assembled with lipids from GELNs (2 mg/mouse). Mice were killed 6 h after the last treatment and β-galactosidase activity was determined by staining fresh intestine with X-gal substrate. Characterization of X-

gal stained whole intestine (Figure 5g) and intestinal tissue sections (Figure 5h) demonstrated that expression of the β-galactosidase is higher in mice treated with the LLNs assembled with lipids from GELNs when compared to mice treated with GELN lipids or vehicle (acetone).

**Oral administration of GELNs protects mice against DSS induced colitis**

Intestinal stem cells have a crucial role in regulating intestinal epithelial cell differentiation and are required for intestinal tissue homeostasis and repair. Since GELNs can induce $Lgr5^{+}$ intestine stem cells, we questioned whether oral administration of GELNs could be used as a therapeutic agent to reduce colitis injury. Lgr5–EGFP–ires–CreERT2 mice given 3% DSS were randomized and received vehicle (PBS) or GELNs (2 mg/mouse) daily. When mice were treated with GELNs, a striking improvement of the wasting disease became apparent (Figure 6a). When 3% DSS was continuously given to control mice and GELN fed mice, within 13 days there was 100% mortality of the control group (Figure 6b), whereas it took 25 days for 100% mortality of the GELN fed mice. During the same time period mice given GELNs once daily had a mortality that was significantly lower within each given date in comparison with that of mice treated with PBS (Figure 6b). Withdrawing administration of the 3% DSS at day 9 led to a rapid decrease and halting of mortality in mice treated with GELNs. GELN treatment prevented DSS induced progression of disease as evidenced by the fact that there was little reduction in intestine length at day 7 post administration of 3% DSS (Figure 6c). Histologic examination showed a comparable villus height of mice treated

with GELNs when compared to naïve mice (Figure 6d); there was a significant decrease in villus height in mice treated with GELN vehicle (PBS).

Given that intestinal stem cell and epithelial cell proliferation activity in re-epithelization is essential for protecting mice against colitis, we then analyzed intestinal epithelial cell proliferation by immunohistological staining of a cell proliferation marker, Ki67, in intestinal tissue of Lgr5-EGFP-IRES-CreERT2 mice. Treatment with GELNs remarkably increased the number of $Lgr5^{+}Ki67^{+}$ double positive stem cells (GELNs/naïve=3.3-fold or GELNs/PBS=4.3-fold) across all segments of the intestine tested as compared with naïve or vehicle treated (PBS) mice(Figure 6e).

We further sought to determine whether oral administration of GELN causes activation of β-catenin and up-regulation of genes that promote intestinal stem cell proliferation under DSS induced pathological conditions. The results of real-time PCR demonstrated that treatment with GELNs enhances the expression of genes that serve as markers of intestinal stem cells (Lgr5, BMI1) and genes that regulate stem cell growth and proliferation as listed in the figure 6f. Immunohistological staining of β-catenin further indicated that treatment with GELNs promotes β-catenin nucleus translocation (Figure 6g) of intestinal epithelia and this result is consistent with the increased phosphorylation of GSK-3β that is a consequence of β-catenin activation. This result was further confirmed with western blot analysis of phosphorylated GSK-3β (supplementary Figure 5).

## Discussion

In this study, exosome-like nanoparticles were identified for the first time from an edible plant, i.e., grapes. Although these nanoparticles may be not identical to mammalian cell derived exosomes, the nano-sized vesicle structure and composition of grape nanoparticles is similar to mammalian derived exosomes based on our characterization. Both grape derived exosome-like nanoparticles and mammalian derived exosomes share certain proteins including HSP70 and aquaporin proteins, lipids enriched for PA and PE. Further study showed that GELNs have unique transport properties and biological functions. We found that grape exosome-like nanoparticles (GELNs) can travel within the gut, migrate through the intestinal mucus, be taken up by mouse intestinal stem cells and subsequently promote the proliferation of intestinal stem cells.

Using grape derived exosome-like nanoparticles as an example, we demonstrated that GELNs remarkably increase the proliferation of $Lgr5^{hi}$ intestinal stem cells under physiological conditions. It has been reported that only the $Lgr5^{hi}$ intestinal stem cells yield long-lived intestinal organoid structures in vitro. Genetic lineage tracing has demonstrated that intestinal stem cells highly expressing Lgr5 contribute to all intestinal lineages throughout life[21, 35]. Under pathological conditions, GELNs also effectively induced proliferation of intestinal stem cells as we demonstrated in this study. In the DSS induced mouse colitis model, GELNs promoted dramatic proliferation of intestinal stem cells and led to an intense acceleration of mucosal epithelium regeneration and a rapid restoring of the intestinal architecture throughout the entire length of the intestine. Furthermore, the current study implies that *in vitro* expansion of gastrointestinal stem

cells may be a promising option for patients with severe gastrointestinal epithelial injuries although further research and optimization is clearly needed**.** In addition, Lgr5 is not restricted to expression on intestinal stem cells but is also present on other tissue derived stem cells. Our data showed that grape nanoparticles are taken up by $Lgr5^+$ intestinal stem cells, leading to their proliferation. Therefore, in principal, grape exosome-like nanoparticle mediated expansion of $Lgr5^+$ stem cells could potentially be applied to other diseases in which $Lgr5^+$ stem cells play a role in the disease process.

In addition, upon in vitro or in vivo GELNs treatment, expression of genes encoding intestinal stem cell marker BMI1 and pluripotent stem cells markers, including SOX2, Nanog, OCT4, and KLF4 were also significantly upregulated*.* $Lgr5^+$ stem cells are sensitive to canonical Wnt modulation, and contribute robustly to homeostatic regeneration, whereas $Bmi1^+$ stem cells contribute weakly to homeostatic regeneration. A large body of data provides evidence that the control of intestinal stem cell fate, stem cell maintenance, and maturation and proliferation of crypt epithelial cells depends on Wnt signals[38-42]. Results of the present study demonstrate that GELNs taken up by intestinal stem cells triggers the activation of downstream canonical Wnt signals. Therefore, under physiological conditions, the GELNs more likely regulate intestinal homeostatic regeneration via induction of $Lgr5^+$ stem cells. Under pathophysiological conditions like DSS mediated intestinal epithelial damage, GELNs not only induce $Lgr5^+$ stem cells but also might activate $BMI1^+$ stem cells to accelerate regeneration of mucosal epithelium. $SOX2^+$ stem cells are also critical for normal tissue regeneration[43].. Ablation of $SOX2^+$ cells in mice results in a disruption of epithelial

tissue homeostasis and lethality (29,30). We observed that expression of pluripotent stem cell markers SOX2, Oct4, Klf4, and Nanog was induced by GELNs. Thus, $Sox2^{+}$ stem cells induced by GELNs may be involved in epithelial tissue homeostasis of the intestine.

Therefore, our findings reveal that under both homeostatic and injury-induced conditions, GELN treatment is beneficial for regenerating intestinal epithelium, thus protecting mice against DSS induced colitis.

The findings as reported in this study also have a number of applications for future study, including potential use of GELN as a delivery vehicle. Unlike nanoparticles synthesized in vitro, GELNs and liposome-like nanoparticles assembled with lipids from GELNs exhibit no cytotoxicity. Therefore, drug delivery by GELNs or liposome-like nanoparticles could be a novel means to transport small molecule drugs to specifically target tissues or cells in a non–cytotoxic manner. Obviously, producing large quantities of nanoparticles from edible grapes is advantageous for accelerating this technology into clinical settings for treatment of intestinal inflammatory related diseases and maybe others. Also, edible plant derived nanoparticles not only exist in grapes but are present in the many different types of food we eat daily. The nanoparticles we eat daily may have synergistic/additive effects on gut biology, such as regulation of intestinal stem cell proliferation as we have demonstrated in this study. Therefore, our findings may open up a new avenue for studying novel mechanisms underlying edible exosome-like particle mediated gut homeostasis maintained by intestinal stem cells or other intestinal cells through exosome-like nanoparticles in food. Although in this study our data show

that intestinal stem cells take up GELNs, we cannot exclude the possibility that other types of intestinal cells may also take up GELNs. These questions related to this initial finding need to be further addressed in the future study.

We realized that PA is much higher in the GELNs we characterized than what has been reported in other nano particles, and this finding was in the face of including 75% isopropanol in our preparations to inactivate possible enzymatic reactions present during the lipid extraction from grapes or GELNs. Based on the literature, we noticed that most investigators used fresh plants as starting material for extraction of lipids and subsequently used for lipid analysis. In contrast, we used grapes which were purchased from grocery stores, and we do not know whether storage conditions including the period of storage, temperature and others have effects on PA production in grapes and GELNs in the grape. However, the material used in this study represents what people would eat. Whether the storage conditions have an effect on the levels of PA in GELNs needs to be investigated further.

In summary, we have identified nanoparticles from grapes. We show that GELNs are taken up by mouse intestinal stem cells and subsequently strongly promote the proliferation of $Lgr5^{hi}$ intestinal stem cells. Our finding opens a new avenue for further studying the mechanism underlying interspecies communication through edible exosome-like nanoparticles.

## Experimental Procedures

**Isolation and purification of grape exosome-like nanoparticles.** Grapes were washed 3x with water in a plastic bucket. After the final washing, grapes with the skin removed manually were pressed in a cold room, the juice collected and diluted with cold PBS. The collected juice was differentially centrifuged and then centrifuged on a sucrose gradient to isolate and purify the exosome-like nanoparticles[18]. The purified specimens were prepared for cryo-electron microscopy using a conventional procedure[44] and observed using an FEI Tecnai F20 electron microscope operated at 200kV at a magnification of 38,000× and defocus of 2.5 µm. Photomicrographs were taken using a Gatan Ultrascan 4000 CCD camera.

For proteomic analysis, protein concentration of GELNs was determined using the Bio-Rad Protein Quantitation Assay kit with bovine serum albumin as a standard. For all other experiments carried out in this study, immediately after being washed, sucrose purified pellets of GELNs were weighed and then suspended in PBS and expressed as mg of GELNs/ml of PBS.

**Lipidomic analysis:** To extract total lipids from grape or GELNs, both samples were immersed in 1 ml of 75°C isopropanol with 0.01% butylated hydroxytoluene (BHT) for 15 min. Addition of isopropanol and BHT have been known to inhibit PLD activity and minimum oxidation[12, 13], respectively. Then, the immersed samples were mixed with 3.75 ml of chloroform/methanol at a 1:2 ratio (v/v) in borosilicate glass test tubes, before adding 1.25 ml chloroform to the mixed sample and vortexing the mixture. Subsequently, 1.25 ml deinonized water was added and the mixture vortexed again.

The sample was centrifuged at 1000 RPM in a table-top microcentrifuge for 5 min at 22°C. The bottom phased liquid that contained lipids was collected using a Pasteur pipette. Solvent in the collected sample was completely removed via a constant flow of nitrogen gas at 60°C. The lipid composition of GELNs or grape was determined using a triple quadrupole mass spectrometer (an Applied Biosystems Q-TRAP, Applied Biosystems, Foster City, CA). The protocol has been previously described[45]. The data are reported as % of total signal for the molecular species determined after normalization of the signals to internal standards of the same lipid class.

**Crypt isolation and treatment**

Intestines were opened longitudinally and washed with cold PBS. The tissue was chopped into pieces approximately 5 mm in size and further washed with cold PBS. The tissue fragments were then incubated in 2 mM EDTA with PBS for 30 min on ice. After removal of the EDTA solution, the tissue fragments were vigorously suspended using a 10-ml pipette with cold PBS, and the suspension allowed to settle for 5 min. The sediment was resuspended in PBS. The suspended sediment was vigorously resuspended one additional time and centrifuged: the supernatant was enriched for crypts. The crypt fraction was passed through a 70-µm cell strainer (BD Bioscience) to remove residual villous material. Isolated crypts were centrifuged at 300g for 3 min to separate crypts from single cells. The final fraction consisted of essentially pure crypts and was used for culture or single cell dissociation.

Culture crypts: Isolated crypts were counted and pelleted. A total of 500 crypts were mixed with 50 µl of Matrigel (BD Bioscience) and plated in 24-well plates. After polymerization of Matrigel containing GELNs (40 µg $ml^{-1}$), 500 µl of crypt culture medium (Advanced DMEM/F12, Invitrogen) containing growth factors (10–50 ng $ml^{-1}$ EGF, 500 ng $ml^{-1}$ R-spondin and 100 ng $ml^{-1}$ Noggin (Peprotech) was added. On day 6 of culture, half of the crypts were used for RNA isolation and the rest were dissociated with TrypLE express (Invitrogen) plus 2,000U/ml DNase (Sigma) for 30 min at 37°C. Dissociated cells were passed through a 40-µm cell strainer (Celltrix) and washed with PBS. Cells were analyzed by flow cytometry (BD).

**Single stem cell culture and GELN treatment**

For single stem cell cultures, dissociated crypt cells collected using the method as described above were passed through a 40-µm cell strainer (Celltrix) and washed with PBS. $EGFP^{hi}$ cells were sorted using a FACSAria III cell sorter (BD). Sorted cells were collected, pelleted and embedded in Matrigel containing Jagged-1 peptide (1 mM; AnaSpec) and GELNs (40µg $ml^{-1}$) and then seeded into a 96-well plate (30–50 singlets; 10 µl Matrigel per well). Culture medium (Advanced DMEM/F12 supplemented with penicillin/streptomycin, 10mM HEPES, Glutamax, 1×N2, 1×B27 (all from Invitrogen) and 1 µM N-acetylcysteine (Sigma)) containing growth factors (50 ng $ml^{-1}$ EGF, 100 ng $ml^{-1}$ noggin, 1 µg $ml^{-1}$ R-spondin) was overlaid on the Matrigel. Y-27632 (10 mM) was included for the first 2 days to avoid anoikis. Growth factors were added every other day and all the medium was changed every 4 days. Cultured cells were manually inspected

using an inverted microscopy and the number of viable organoids in triplicate wells was calculated.

To determine the efficiency of colony formation, Lgr5EGFP$^{+}$ cells from different treatment groups were cultured in 96-well plates. Eleven days after plating, spheres with a diameter over 40 μm were counted, and colony forming efficiency was calculated (Percentage of colonies = Number of colonies formed / Number of cells inoculated × 100%). All experiments were repeated at least three times.

**In vivo up taking GELNs**

To determine whether Lgr5$^{+}$ intestinal stem cells take up GELNs, Lgr5-EGFP-IRES-CreERT2 mice starved overnight were given 1 mg PKH26 (Sigma) fluorescent dye labeled GELNs/mouse by gavage in 100 μl of PBS. 6 h after gavaging, mice were sacrificed and intestinal tissues were embedded in OCT compound (Miles Laboratories; Elkhart, IN) and frozen. Tissues were sectioned 5 μm thick with a cryostat and mounted on commercially provided charged slides (Fisher Scientific; Pittsburgh, PA) for immunohistological and DAPI (Molecular Probe) staining. Images were acquired with a Zeiss LSM 510 confocal microscope equipped with a digital image analysis system (Pixera) and quantified by counting the number of stained nuclei in five individual fields for each slide.

**Liposome-like nanoparticles assembling**

Liposome-like nanoparticles were assembled according to the method described [46, 47] with a minor modification. 1 ml of GELNs in PBS were mixed together with 3.75 ml of chloroform/methanol at a 1:2 ratio (v/v) in borosilicate glass test tubes, before adding 1.25 ml chloroform to the mixed sample and vortexing the mixture. Subsequently, 1.25 ml deinonized water was added and the mixture vortexed again. The sample was centrifuged at 1000 RPM in a table-top microcentrifuge for 5 min at 22°C. The bottom phased liquid that contained lipids was collected using a pasteur pipette. Solvent in the collected sample was completely removed via a constant flow of nitrogen gas at 60°C. Extracted GELN lipids were hydrated with 800µl of Milli-Q water prior to bath sonication for 3 min, and then sonicated for an additional 2 min after addition of HEPES buffered saline (final contration,10 mM Hepes, 50 mM NaCl). This resulted in a clear dispersion being produced that was stored at 4°C for 48 h prior to further experimentation or examination for liposome-like nanoparticle formation using a conventional procedure[48].

**Liposome-like nanoparticles (LLNs) treatment**

All LLN related experiments were performed using identical protocols as described for GELN related experiments. Identical amounts of GELNs used for GELN related experiments were also used for LLN experiments including an in vivo PKH26 labeled LLN confocal microscopy of Lgr5EGP$^{+}$ stem cells in Lgr5-EGFP-IRES-CreERT2 mice, activation of β-catenin in B6.Cg-Tg(BAT-lacZ)3Picc/J mice, in vitro effects of LLNs on the induction of LGR5EGFP$^{+}$ cells in cultured intestinal crypts of Lgr5-EGFP-IRES-CreERT2 mice, and treatment of the CT26 cell line.

**DSS induced colitis.**

Colitis was induced using dextran sulfate sodium (DSS) with a molecular weight of 36,000-50,000 (MP Biomedicals) to prepare a 3% solution that was provided to male mice (18–25 g, 6 weeks old) in drinking water. Other protocols including SDS PAGE analysis of GELN proteins have been described previously[18, 49]. Details of other methods used in this study are described in the supplemental experimental procedures.

**Statistical analysis**. Survival data were analyzed using the log rank test. The Student's *t*-test was used for comparison of two samples with unequal variances. One-way ANOVA with Holm's *post hoc* test was used for comparing means of three or more variables.

**Acknowledgments**

We thank Dr. Jerald Ainsworth for editorial assistance. This work was supported by grants from the National Institutes of Health (NIH)(RO1CA137037, R01CA107181, RO1AT004294, and RO1CA116092); the Louisville Veterans Administration Medical Center (VAMC) Merit Review Grants (H.-G.Z.); a grant from the Susan G. Komen Breast Cancer Foundation. Instrument acquisition and method development at the Kansas Lipidomics Research Center was supported by grants from the National Science Foundation (EPS 0236913, DBI 0521587, DBI 1228622, and MCB 0920663), Kansas Technology Enterprise Corporation, K-IDeA Networks of Biomedical Research

Excellence (INBRE) of National Institute of Health (P20RR16475), and Kansas State University

References:

1. Johnstone, RM, Adam, M, Hammond, JR, Orr, L, and Turbide, C (1987). Vesicle formation during reticulocyte maturation. Association of plasma membrane activities with released vesicles (exosomes). *J Biol Chem* **262**: 9412-9420.
2. Wolfers, J*, et al.* (2001). Tumor-derived exosomes are a source of shared tumor rejection antigens for CTL cross-priming. *Nature medicine* **7**: 297-303.
3. Valadi, H, Ekstrom, K, Bossios, A, Sjostrand, M, Lee, JJ, and Lotvall, JO (2007). Exosome-mediated transfer of mRNAs and microRNAs is a novel mechanism of genetic exchange between cells. *Nat Cell Biol* **9**: 654-659.
4. Zhang, HG*, et al.* (2006). A membrane form of TNF-alpha presented by exosomes delays T cell activation-induced cell death. *Journal of immunology* **176**: 7385-7393.
5. Liu, C*, et al.* (2006). Murine mammary carcinoma exosomes promote tumor growth by suppression of NK cell function. *Journal of immunology* **176**: 1375-1385.
6. Thery, C, Ostrowski, M, and Segura, E (2009). Membrane vesicles as conveyors of immune responses. *Nature reviews Immunology* **9**: 581-593.
7. An, Q, Huckelhoven, R, Kogel, KH, and van Bel, AJ (2006). Multivesicular bodies participate in a cell wall-associated defence response in barley leaves attacked by the pathogenic powdery mildew fungus. *Cell Microbiol* **8**: 1009-1019.
8. Regente, M, Pinedo, M, Elizalde, M, and de la Canal, L (2012). Apoplastic exosome-like vesicles: A new way of protein secretion in plants? *Plant Signal Behav* **7**.
9. Nielsen, ME, Feechan, A, Bohlenius, H, Ueda, T, and Thordal-Christensen, H (2012). Arabidopsis ARF-GTP exchange factor, GNOM, mediates transport required for innate immunity and focal accumulation of syntaxin PEN1. *Proceedings of the National Academy of Sciences of the United States of America*.
10. Wei, T, Hibino, H, and Omura, T (2009). Release of Rice dwarf virus from insect vector cells involves secretory exosomes derived from multivesicular bodies. *Commun Integr Biol* **2**: 324-326.
11. Xiang, X*, et al.* (2010). TLR2-mediated expansion of MDSCs is dependent on the source of tumor exosomes. *Am J Pathol* **177**: 1606-1610.
12. Guo, L*, et al.* (2012). Connections between sphingosine kinase and phospholipase D in the abscisic acid signaling pathway in Arabidopsis. *J Biol Chem* **287**: 8286-8296.
13. Peters, C, Li, M, Narasimhan, R, Roth, M, Welti, R, and Wang, X (2010). Nonspecific phospholipase C NPC4 promotes responses to abscisic acid and tolerance to hyperosmotic stress in Arabidopsis. *Plant Cell* **22**: 2642-2659.
14. Wang, YY, Lai, SK, So, C, Schneider, C, Cone, R, and Hanes, J (2011). Mucoadhesive nanoparticles may disrupt the protective human mucus barrier by altering its microstructure. *PLoS One* **6**: e21547.
15. Cone, RA (2009). Barrier properties of mucus. *Adv Drug Deliv Rev* **61**: 75-85.

16. Lai, SK*, et al.* (2011). Drug carrier nanoparticles that penetrate human chronic rhinosinusitis mucus. *Biomaterials* **32**: 6285-6290.
17. Lai, SK, Wang, YY, and Hanes, J (2009). Mucus-penetrating nanoparticles for drug and gene delivery to mucosal tissues. *Adv Drug Deliv Rev* **61**: 158-171.
18. Zhuang, X*, et al.* (2011). Treatment of Brain Inflammatory Diseases by Delivering Exosome Encapsulated Anti-inflammatory Drugs From the Nasal Region to the Brain. *Mol Ther* **19**: 1769-1779.
19. Huss, M*, et al.* (2002). Concanamycin A, the specific inhibitor of V-ATPases, binds to the V(o) subunit c. *J Biol Chem* **277**: 40544-40548.
20. Niikura, K (2006). Vacuolar ATPase as a drug discovery target. *Drug News Perspect* **19**: 139-144.
21. Sato, T*, et al.* (2009). Single Lgr5 stem cells build crypt-villus structures in vitro without a mesenchymal niche. *Nature* **459**: 262-265.
22. Naro, F, Donchenko, V, Minotti, S, Zolla, L, Molinaro, M, and Adamo, S (1997). Role of phospholipase C and D signalling pathways in vasopressin-dependent myogenic differentiation. *J Cell Physiol* **171**: 34-42.
23. Grange, M*, et al.* (2000). The cAMP-specific phosphodiesterase PDE4D3 is regulated by phosphatidic acid binding. Consequences for cAMP signaling pathway and characterization of a phosphatidic acid binding site. *J Biol Chem* **275**: 33379-33387.
24. van Es, JH*, et al.* (2012). A Critical Role for the Wnt Effector Tcf4 in Adult Intestinal Homeostatic Self-Renewal. *Mol Cell Biol*.
25. Kim, TH, Escudero, S, and Shivdasani, RA (2012). Intact function of Lgr5 receptor-expressing intestinal stem cells in the absence of Paneth cells. *Proceedings of the National Academy of Sciences of the United States of America* **109**: 3932-3937.
26. Fauser, JK*, et al.* (2011). Wnt Blockade With Dickkopf Reduces Intestinal Crypt Fission And Intestinal Growth In Infant Rats. *J Pediatr Gastroenterol Nutr*.
27. Yan, KS*, et al.* (2012). The intestinal stem cell markers Bmi1 and Lgr5 identify two functionally distinct populations. *Proceedings of the National Academy of Sciences of the United States of America* **109**: 466-471.
28. Birchmeier, W (2011). Stem cells: Orphan receptors find a home. *Nature* **476**: 287-288.
29. de Lau, W*, et al.* (2011). Lgr5 homologues associate with Wnt receptors and mediate R-spondin signalling. *Nature* **476**: 293-297.
30. Marsh, V*, et al.* (2008). Epithelial Pten is dispensable for intestinal homeostasis but suppresses adenoma development and progression after Apc mutation. *Nat Genet* **40**: 1436-1444.
31. Jiang, S*, et al.* (2008). Hematopoietic stem cells contribute to lymphatic endothelium. *PLoS One* **3**: e3812.
32. de la Roche, M*, et al.* (2012). An intrinsically labile alpha-helix abutting the BCL9-binding site of beta-catenin is required for its inhibition by carnosic acid. *Nat Commun* **3**: 680.
33. Itzkovitz, S*, et al.* (2012). Single-molecule transcript counting of stem-cell markers in the mouse intestine. *Nature cell biology* **14**: 106-114.
34. Zeki, SS, Graham, TA, and Wright, NA (2011). Stem cells and their implications for colorectal cancer. *Nat Rev Gastroenterol Hepatol* **8**: 90-100.
35. Snippert, HJ*, et al.* (2010). Intestinal crypt homeostasis results from neutral competition between symmetrically dividing Lgr5 stem cells. *Cell* **143**: 134-144.
36. Barker, N*, et al.* (2010). Lgr5(+ve) stem cells drive self-renewal in the stomach and build long-lived gastric units in vitro. *Cell Stem Cell* **6**: 25-36.
37. van der Flier, LG*, et al.* (2009). Transcription factor achaete scute-like 2 controls intestinal stem cell fate. *Cell* **136**: 903-912.

38. Cheasley, D, Pereira, L, Lightowler, S, Vincan, E, Malaterre, J, and Ramsay, RG (2011). Myb controls intestinal stem cell genes and self-renewal. *Stem Cells* **29**: 2042-2050.
39. Shin, K*, et al.* (2011). Hedgehog/Wnt feedback supports regenerative proliferation of epithelial stem cells in bladder. *Nature* **472**: 110-114.
40. Takashima, S*, et al.* (2011). The Wnt agonist R-spondin1 regulates systemic graft-versus-host disease by protecting intestinal stem cells. *J Exp Med* **208**: 285-294.
41. Spence, JR*, et al.* (2011). Directed differentiation of human pluripotent stem cells into intestinal tissue in vitro. *Nature* **470**: 105-109.
42. Sato, T*, et al.* (2011). Paneth cells constitute the niche for Lgr5 stem cells in intestinal crypts. *Nature* **469**: 415-418.
43. Yan, KS*, et al.* (2012). The intestinal stem cell markers Bmi1 and Lgr5 identify two functionally distinct populations. *Proc Natl Acad Sci U S A* **109**: 466-471.
44. Spilman, MS, Welbon, C, Nelson, E, and Dokland, T (2009). Cryo-electron tomography of porcine reproductive and respiratory syndrome virus: organization of the nucleocapsid. *J Gen Virol* **90**: 527-535.
45. Xiao, S*, et al.* (2010). Overexpression of Arabidopsis acyl-CoA binding protein ACBP3 promotes starvation-induced and age-dependent leaf senescence. *Plant Cell* **22**: 1463-1482.
46. Laulagnier, K*, et al.* (2004). Mast cell- and dendritic cell-derived exosomes display a specific lipid composition and an unusual membrane organization. *Biochem J* **380**: 161-171.
47. Bligh, EG, and Dyer, WJ (1959). A rapid method of total lipid extraction and purification. *Can J Biochem Physiol* **37**: 911-917.
48. Wang, GJ*, et al.* (2008). Thymus exosomes-like particles induce regulatory T cells. *Journal of immunology* **181**: 5242-5248.
49. Liu, Y*, et al.* (2010). Contribution of MyD88 to the tumor exosome-mediated induction of myeloid derived suppressor cells. *Am J Pathol* **176**: 2490-2499.

## Figure Legends

**Figure 1: Identification and characterization of grape exosome-like nanoparticles (GELNs).** Grape exosome-like nanoparticles (GELNs) were isolated using differential centrifugation and sucrose gradient ultracentrifugation. (a) Electron photomicrographs of GELNs. The sucrose-gradient band indicated by the arrow (left) was collected for EM examination and the image (right) shows small vesicles of 50-300 nm in diameter. The scale bar indicates 200 nm. (b) Size distribution of the GELNs was further analyzed using the Zeta potential Analyzer. (c) The lipids extracted from intestinal-derived

exosomes and GELNs were separated on a thin-layer chromatography plate and developed by spraying the plate with a 10% copper sulfate and 8% phosphoric acid solution. A representative image was scanned using an Odyssey Scanner. (d) Pie chart with a summary of the putative lipid species in GELNs, reported as percent of total GELN lipids. Major details are reported in Supplemental Table S2 in the Supporting Information. PA: Phosphatidic acids; PS: Phosphatidylserine; PI: Phosphatidylinositol; PE: Phosphatidylethanolamines; PC: Phosphatidylcholines; PG:Phosphatidylglycerol; LPE: Lyso-Phosphatidylethanolamines; LPC: Lyso-Phosphatidylcholines; LPG: Lyso-Phosphatidylglycerol; MG/DG: Mono/Di/ glycerols. (e*)* GELN RNA treated with/without RNAase was run on a 2% agarose gel stained with ethidium bromide. Results (a-c, e) represent one of four independent experiments.

**Figure 2: Grape exosome-like nanoparticles are taken up by intestinal stem cells.**

(a) In vivo imaging of trafficking of GELNs. Female C57BL/6 mice were gavage administered DiR dye labeled GELNs (1mg per mouse in 200 µl PBS) and imaged over 48 h (left), and followed by graphical figure (right) presented as mean of net intensity (Sum Intensity/Area, n=5). (b) Intestinal stem cells taking up PKH26 labeled GELNs. Lgr5–EGFP–ires–CreERT2 mice were starved overnight and then gavage administered PKH26-GELNs (1mg per mouse in 200 µl PBS). At 6h after the administration, $PKH26^{+}$/Lgr5-$EGFP^{+}$ cells in frozen sections of intestine were examined by confocal microscopy (left) and were quantified (right). Original magnification was ×40 (left panels) with enlargement of the indicated area shown in the right panels. (c) The intestinal

epithelial CT26 cell line taking up PKH26 labeled GELNs. The CT26 cell line was serum-starved for 6h and then cultured in the presence of PKH26 dye labeled GELNs (20 μg/ml) for 3h. The treated CT26 cells were washed, fixed, and stained with anti-EPCAM antibody, followed by Alexa Fluor® 488 conjugated goat anti-rat IgG secondary antibody. Original magnification was ×40 (left panel) with enlargement of the indicated area shown in the right panel. (d) Blocking of CT26 uptake of PKH26 labeled GELNs. CT26 cells were incubated with the indicated chemical reagents or PBS as a control in the presence of PKH26 labeled GELNs (20 μg/ml) for 3 h. The treated cells were then washed, fixed, and $PKH26^+$ cells were analyzed by FACS. Results (a-d) represent one of five independent experiments (n=3). (e) A fragment of colon tissue of Lgr5–EGFP–ires–CreERT2 mice were treated with PKH26 dyed labeled GELNs (20 μg/ml) in the presence of cytochalasin D (1 μM) for 12 h at 37°C. Treated tissue was frozen sectioned, stained with DAPI, and $PKH26^+EGFP^+$ cells, and $PKH26^-EGFP^+$ cells were examined by confocal microscopy (left) and were quantified (right), and the data were expressed as % = numbers of $PKH26^+EGFP^+/EGFP^+$ x100.

**Figure 3: GELNs induce the proliferation of intestinal stem cells.** Lgr5–EGFP–ires–CreERT2 mice or C57BL/6j mice were gavage administered GELNs (2mg per mouse in 200 μl PBS) or a vehicle (PBS) every day for 7 days, and were sacrificed at day 7. (a) Lgr5-EGFP and Ki67 expression in intestinal crypts of Lgr5–EGFP–ires–CreERT2 mice $PKH26^-EGFP^+$ cells were examined by confocal microscopy (left) and were quantified (right). Magnification 60×. The arrow head indicates Lgr5-$EGFP^+Ki67^+$ cells. (b) Intestinal crypts were isolated and cells dissociated as described in the materials and

methods. FACS analysis of the percentage of Lgr5-EGFP$^{+}$ cells in intestinal crypts. One representative example of six independent experiments is shown (Left), and statistical analysis shows that the Lgr5-EGFP$^{hi}$ subset percentage was significantly higher in the GELN treated mice (n=6) (right). (c) Real-time PCR analysis mRNA expression of Lgr5 in the tissue of the small intestine from C57BL/6j. The results represent the mean ± SEM of three independent experiments. (d) GELNs (40µg/ml) induce growth of crypts *ex vivo* in an intestinal crypt culture system. Magnification 20×. One representative example of five independent experiments is shown. (e) GELNs enhance the proliferation of Lgr5-EGFP$^{+}$ intestinal stem cells in the *ex vivo* cultured crypts. Cultured crypts were collected at day 6 and dissociated with TrypLE express as described in the materials and methods. FACS analysis of the percentage of Lgr5-EGFP$^{+}$ cells in the cultured intestinal crypts. One representative of four independent experiments is shown (left), and the percentage of Lgr5-EGFP$^{+}$ cells was FACS analyzed (right). (f) GELNs enhance the formation of crypt organoids in the *ex vivo* culture system from a single isolated Lgr5-EGFP$^{+}$ stem cell. Magnification 40×. One representative example of four independent experiments is shown.

**Figure 4: Liposome-like nanoparticles (LLNs) induce the production of intestinal stem cells.** (a) Electron microscopy analysis of LLNs assembled with lipids from GELNs. LLNs were purified from the GELN-lipids assembled using a sucrose gradient and examined using electron microscopy. The photomicrograph is representative of two independent experiments with similar results. (b) Confocal analysis of trace LLNs

assembled with GELN-lipids in the mouse intestine. LLNs assembled with GELN-lipids were labeled with PKH26 dye (red). Lgr5–EGFP–ires–CreERT2 mice were starved overnight and then gavage-administered PKH26 labeled LLNs assembled with GELN-lipids (1mg per mouse in 200 µl PBS). Mice were sacrificed 6h after the treatment. Samples taken from the middle of the small intestine were embedded in OCT compound and sliced at 5 µm thickness using a cryostat. Tissues were counter stained with DAPI (blue). Magnification 60×. The arrowhead indicates LLNs assembled with GELN-lipid taken up by Lgr5-EGFP$^{+}$ cells. PKH26$^{+}$EGFP$^{+}$ cells were examined by confocal microscopy (left) and were quantified (right), and the data were expressed as % = numbers of PKH26$^{+}$EGFP$^{+}$/EGFP$^{+}$ x100. (c) LLNs assembled with GELN-lipids enhance the proliferation of Lgr5-EGFP$^{+}$ intestinal stem cells in *ex vivo* cultured crypts. Cultured crypts in the present of LLNs assembled with GELN-lipids were collected at day 6 and dissociated with TrypLE express as described in the materials and methods. FACS analysis of the percentage of Lgr5-EGFP$^{+}$ cells (n=5) in the cultured intestinal crypts. One representative of four independent experiments is shown (left), and the percentage of Lgr5-EGFP$^{+}$ cells was FACS analyzed (right). (d) Real-time analysis of the expression of different genes induced by LLNs assembled with GELN-lipids (40 µg/ml) in *ex vivo* cultured crypts at day 6. Error bars (b-d) represent the mean ± SEM of duplicate experiments (n=5). (e) GELNs were pretreated with or without the propranolol (0, 5µM, 20 µM) for 30 min, and sucrose purified GELNs (1.0 µM) were then added to C57BL/6 intestinal tissues in a 6-well cell culture plate, and cultured for 6, 12 and 18 h. Ki67 Immunofluorescence staining of C57BL/6 intestinal tissues was carried out. A representative example of 12 h cultured C57BL/6 intestinal tissue sections stained with

anti-Ki67 (red) and nuclei (blue, DAPI) are shown (left). The results represent the mean ± SEM of three independent experiments (right).

**Figure 5: GELN treatment stimulates activation of the Wnt/β-catenin pathway and enhances expression of stem cell growth related genes.**

(a) Tcf/LEF activation was detected by X-gal staining (blue) of sectioned intestine of B6.Cg-Tg(BAT-lacZ)3Picc/J mice daily administered 2 mg/mouse GELNs for 7 days by oral gavage. Sections were counter stained with nuclear fast red (red). Original magnification was ×40 (left panels) with enlargement of the indicated area shown in the right panels. (b) Real-time analysis of expression of different genes in single Lgr5-EGFP$^{hi}$ stem cells isolated from Lgr5–EGFP–ires–CreERT2 mice daily administered 2 mg/mouse GELNs for 7 days by oral gavage. (c) CT26 cells serum-starved for 6h and then stimulated with GELNs (40 μg/ml), Carnosic acid (20 μg/ml), or GELNs plus Carnosic acid for 3h. Cells were washed, fixed, permeated and stained with the Alexa Fluor® 488 conjugated-anti-β-catenin, counter stained with DAPI (blue) and analyzed by confocal microscopy for the nuclear translocation of β-catenin (green). Original magnification 40×. (d) Western blot analysis of phosphorylation of GSK-3β (Ser 9) in CT26 cells over time stimulated by GELNs at a dose of 40μg/ml. (e) Canosic acid, a β-catenin inhibitor, partially reverses GELNs mediated-enhancement of the proliferation of Lgr5-EGFP$^{+}$ intestinal stem cells in *ex vivo* cultured crypts. Cultured crypts in the

present of canosic acid (20 μg/ml) were collected at day 6 and dissociated with TrypLE express as described in the materials and methods. One representative of four independent experiments is shown (left), and the percentage of Lgr5-EGFP$^{+}$ cells was FACS analyzed (right). One representative result of at least four independent experiments (a-d) is shown. (f) Real-time analysis of genes expressed in the crypts isolated from C57BL/6 mice; *ex vivo* cultured with GELNs at a dose of 40 μg/ml. Tcf/LEF-reporter mice starved overnight were gavage-administered twice a day for 6 days 2 mg of LLNs assembled with GELN-lipids per mouse in 200 μl PBS or an equal amount of lipid dissolved in acetone. (g) Photographs of X-gal–stained B6.Cg-Tg(BAT-lacZ)3Picc/J mouse intestine after a 3-day treatment. (h) X-gal staining (blue) of sectioned intestine of B6.Cg-Tg(BAT-lacZ)3Picc/J mice. Tissues were counter stained with nuclear fast red (red). Original magnification 40×. One representative example of at least three independent experiments (g, h) is shown.

**Figure 6: Oral administration of GELNs attenuates the severity of colitis induced by DSS**. Lgr5–EGFP–ires–CreERT2 mice were treated for 7 days with 2 mg/mouse of GELNs in 200 μl PBS: (a) GELN treated mice presented with a better body condition. One representative photograph of 5 mice/group of five independent experiments (n= 5) was taken at day 7 after the treatment. (b) Survival analysis. ***p*<0.01 GELNs vs. PBS. Intestinal morphometry of intestinal length (c), and villus height (d). Five mice in each group were sacrificed for the morphometry analysis. One representative analysis of the intestine length (c, left panel) and HE stained section of small intestine (d, left panel) of

three independent experiments (n = 5) is shown. Intestine length was measured by a ruler (c) or villous height was measured by a calibrated eye objective micrometer. Values are mean ± standard error; *$p$<0.05, compared with PBS treated mice (n= 5). (e) $EGFP^+$ and $Ki67^+$cells in frozen sections of intestine were examined by confocal microscopy and quantified (right, n=5). Original magnification was 40× with enlargement of the indicated area (insets). The arrowhead indicates $EGFP^+Ki67^+$ cells. One representative example of at least three independent experiments is shown. (f) Real-time analysis of mRNA expression of different genes in the intestinal crypts from C57BL/6j mice. Values are mean ± standard error. *$p$<0.05, **$p$<0.01 compared with PBS treated mice (N = 5). (g) Confocal analysis of nuclear translocation of β-catenin (top panels) and phosphorylation of GSK-3β (Ser 9) (bottom panels) in the crypt sections from DSS treated C57BL/6j mice. The sections were counterstained with DAPI (blue).

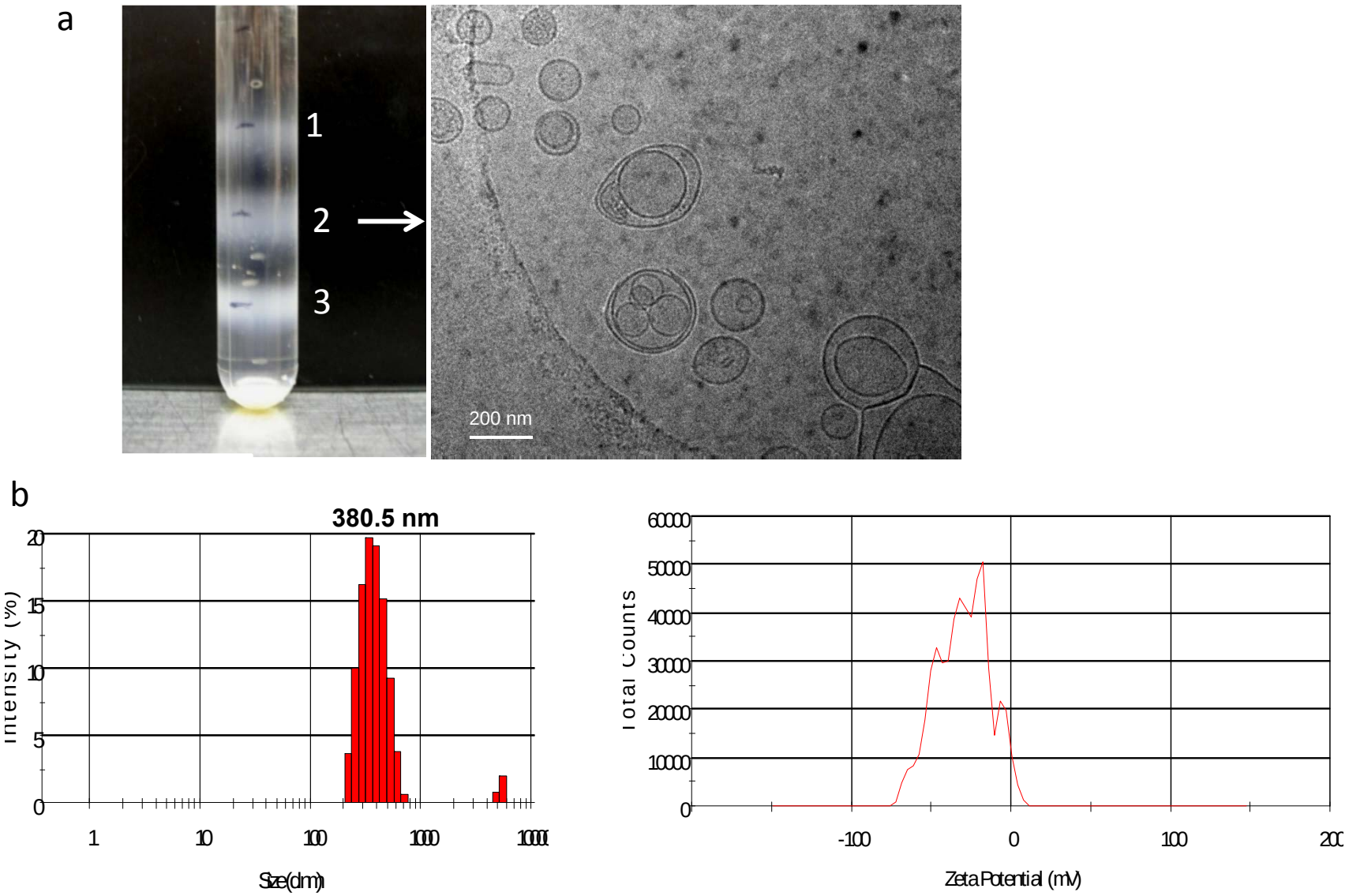
a
1
2
3
200 nm
b
380.5 nm
Intensity (%)
Size(dnm)
Total Counts
Zeta Potential (mV)

Figure 1

c

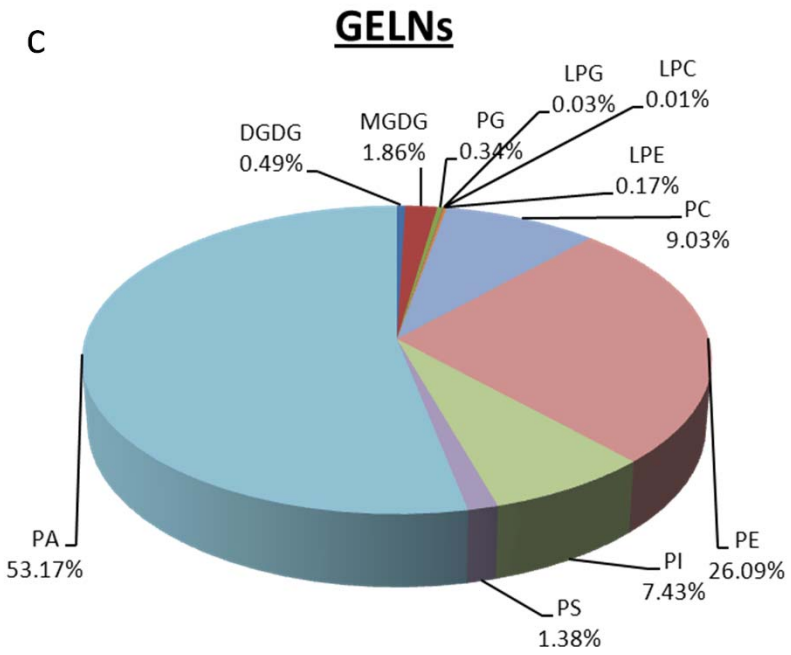
GELNs
LPG
0.03%
LPC
0.01%
DGDG
0.49%
MGDG
1.86%
PG
0.34%
LPE
0.17%
PC
9.03%
PA
53.17%
PE
26.09%
PI
7.43%
PS
1.38%

d

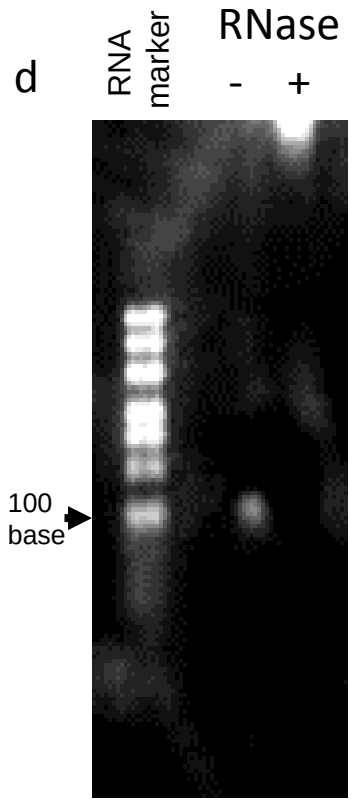
RNA marker
RNase
-
+
100 base

Figure 1

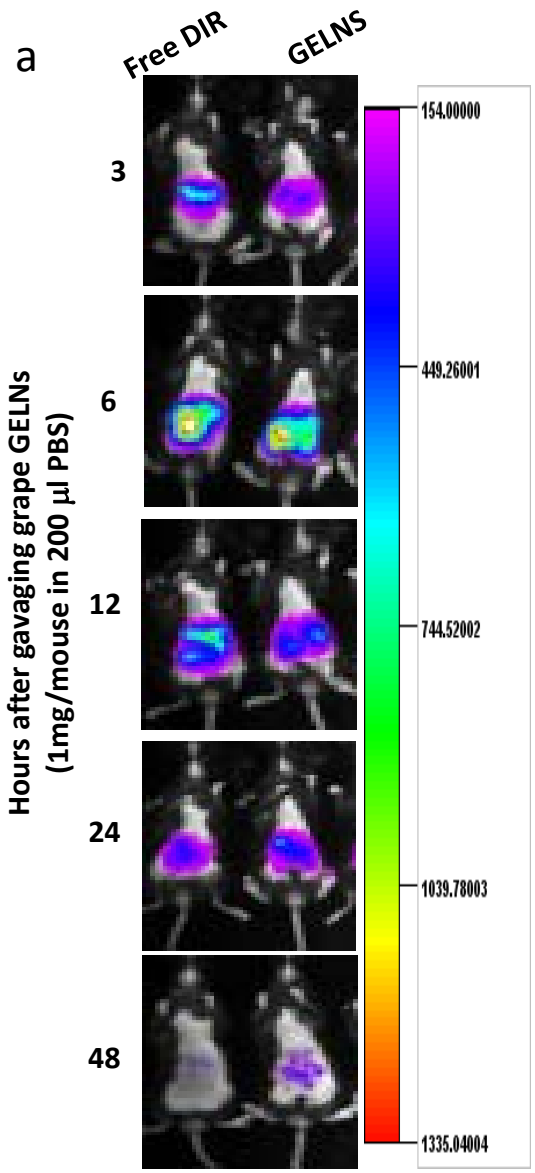
a
Free DIR
GELNS
Hours after gavaging grape GELNs
(1mg/mouse in 200 µl PBS)
3
6
12
24
48
154.00000
449.26001
744.52002
1039.78003
1335.04004

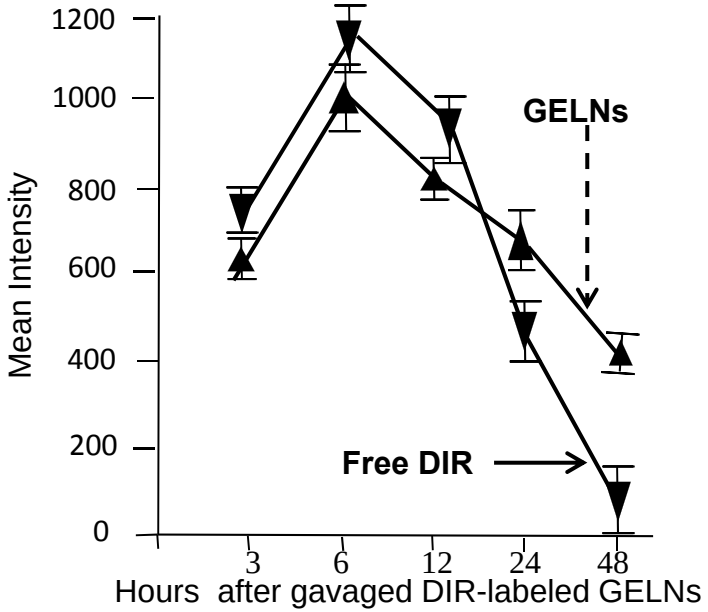
Mean Intensity
1200
1000
800
600
400
200
0
GELNs
Free DIR
3
6
12
24
48
Hours after gavaged DIR-labeled GELNs

Figure 2

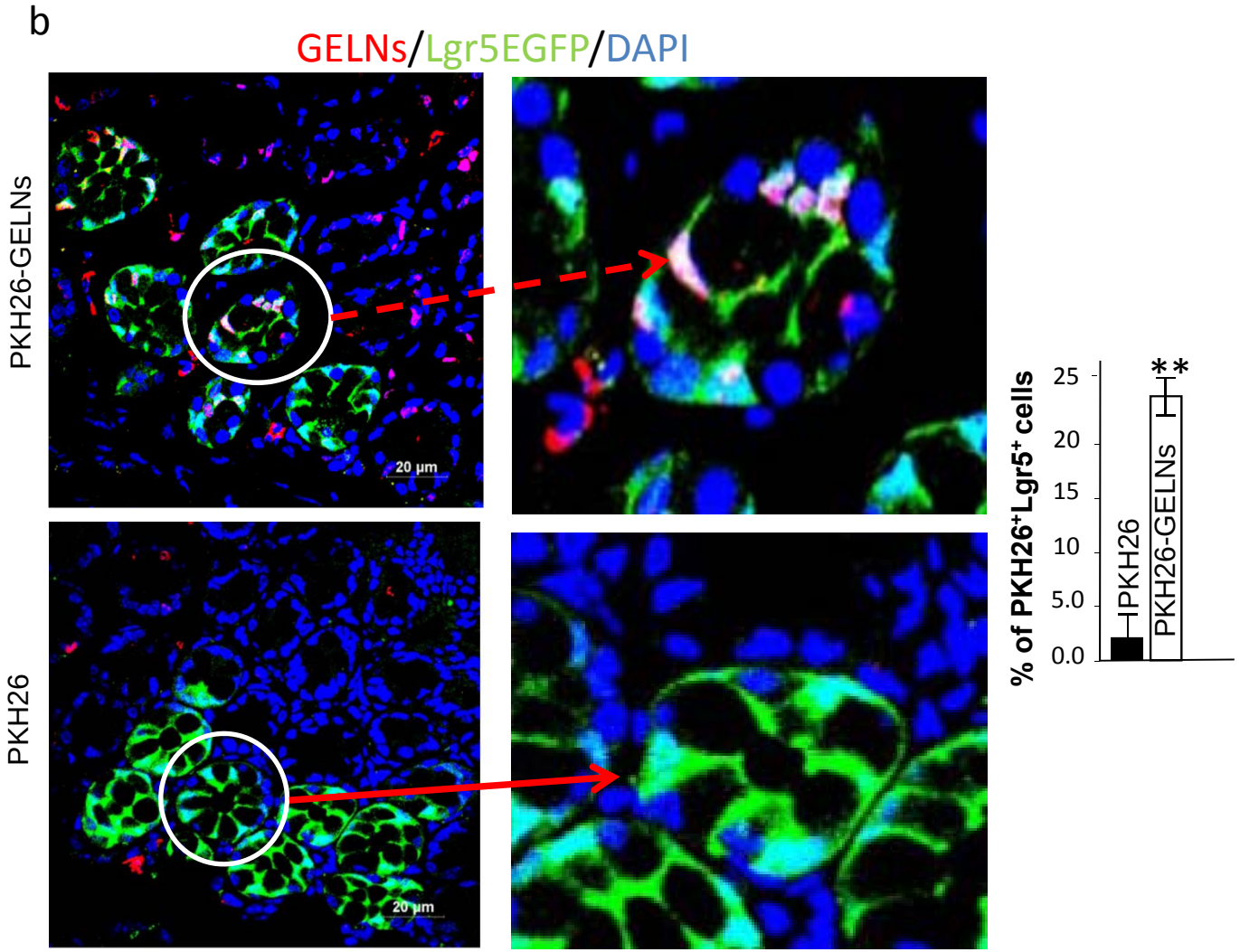
b
GELNs/Lgr5EGFP/DAPI
PKH26-GELNs
PKH26
20 μm
20 μm
% of PKH26+Lgr5+ cells
25
20
15
10
5.0
0.0
PKH26
PKH26-GELNs
**

Figure 2

c

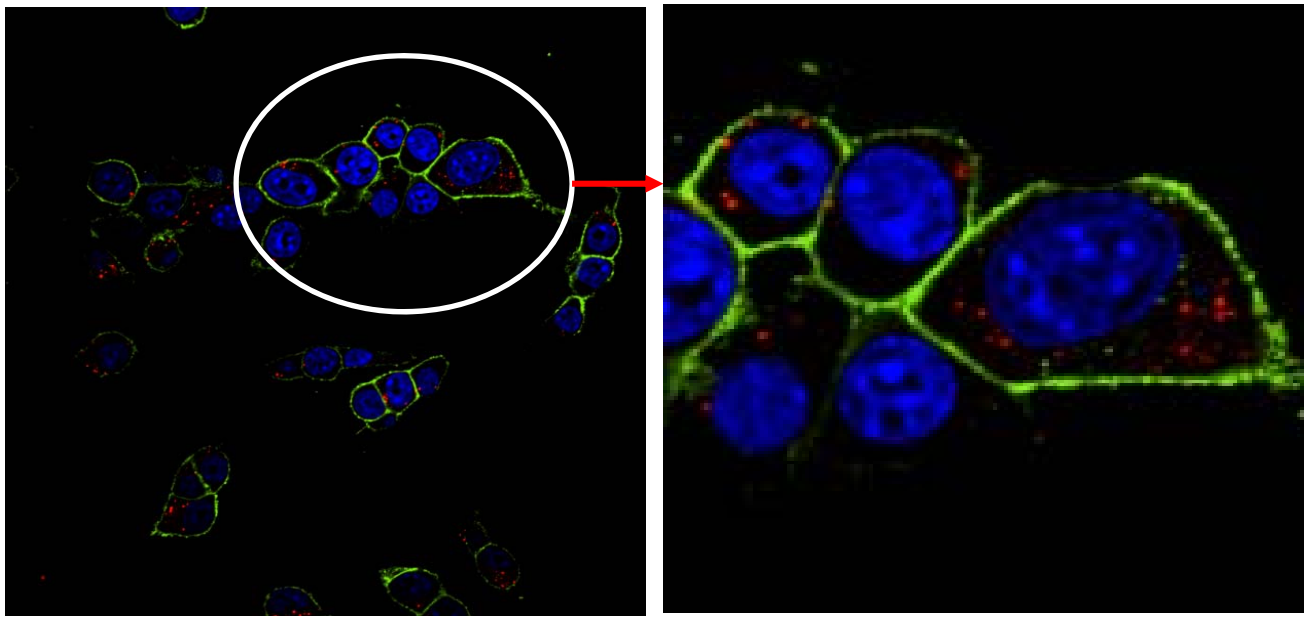
GELNs/EPCAM/DAPI

d

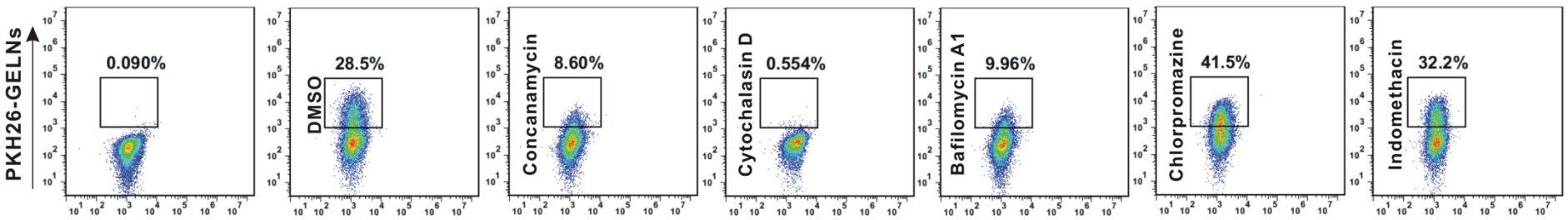
PBS
PKH26-GELNs(20μg/ml for 3h)
PKH26-GELNs
0.090%
DMSO
28.5%
Concanamycin
8.60%
Cytochalasin D
0.554%
Bafilomycin A1
9.96%
Chlorpromazine
41.5%
Indomethacin
32.2%

Figure 2

e

Cytochalasin D (1.0 μM)

\+ GELNs/Lgr5/DAPI -

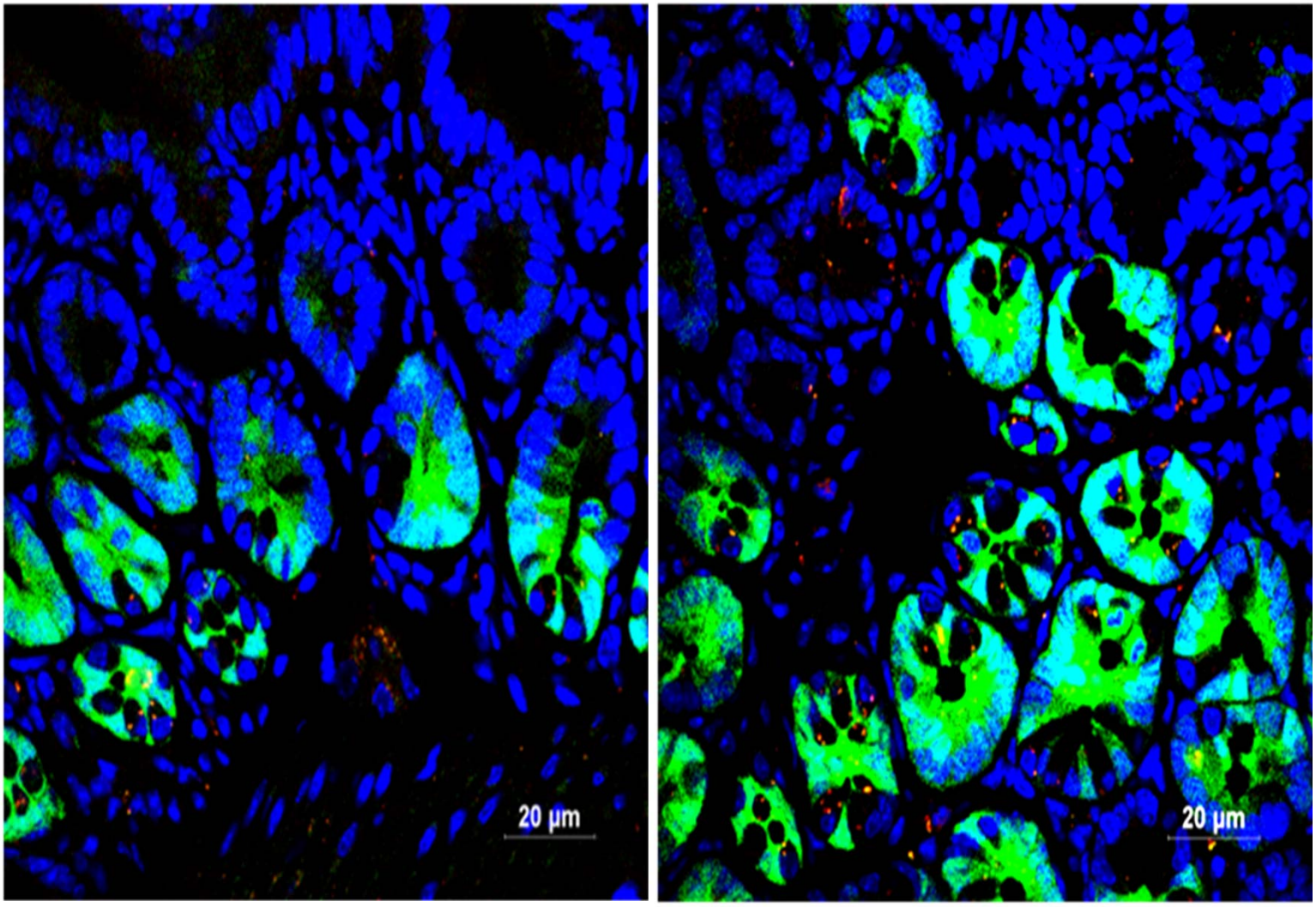


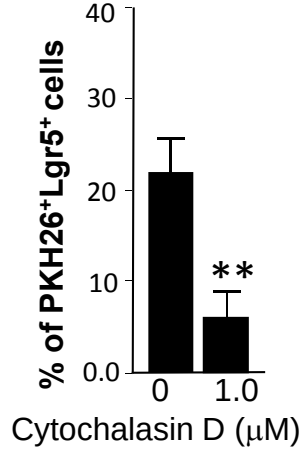

a

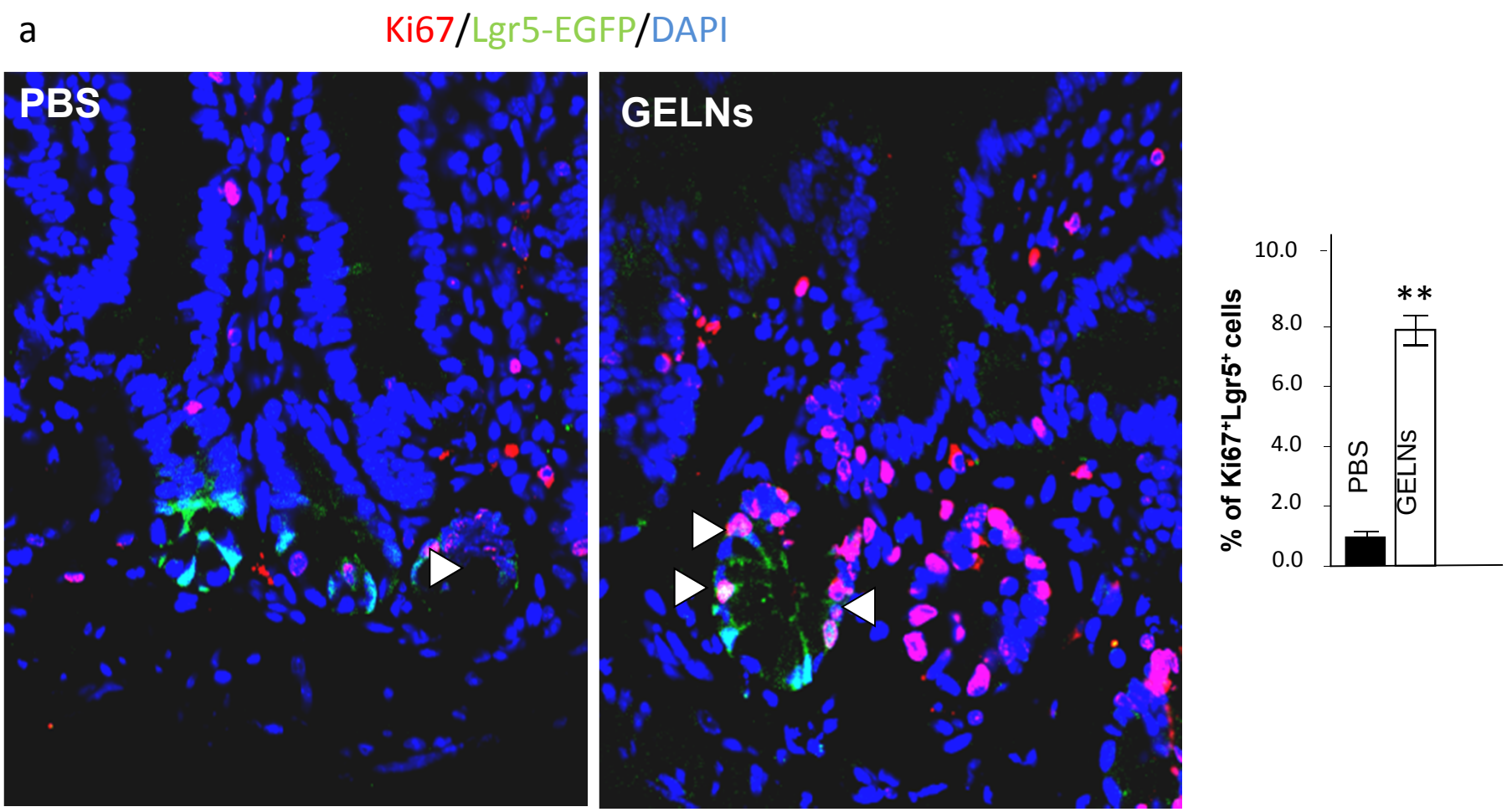
Ki67/Lgr5-EGFP/DAPI
PBS
GELNs
% of Ki67+Lgr5+ cells
10.0
8.0
6.0
4.0
2.0
0.0
PBS
GELNs
**

Figure 3

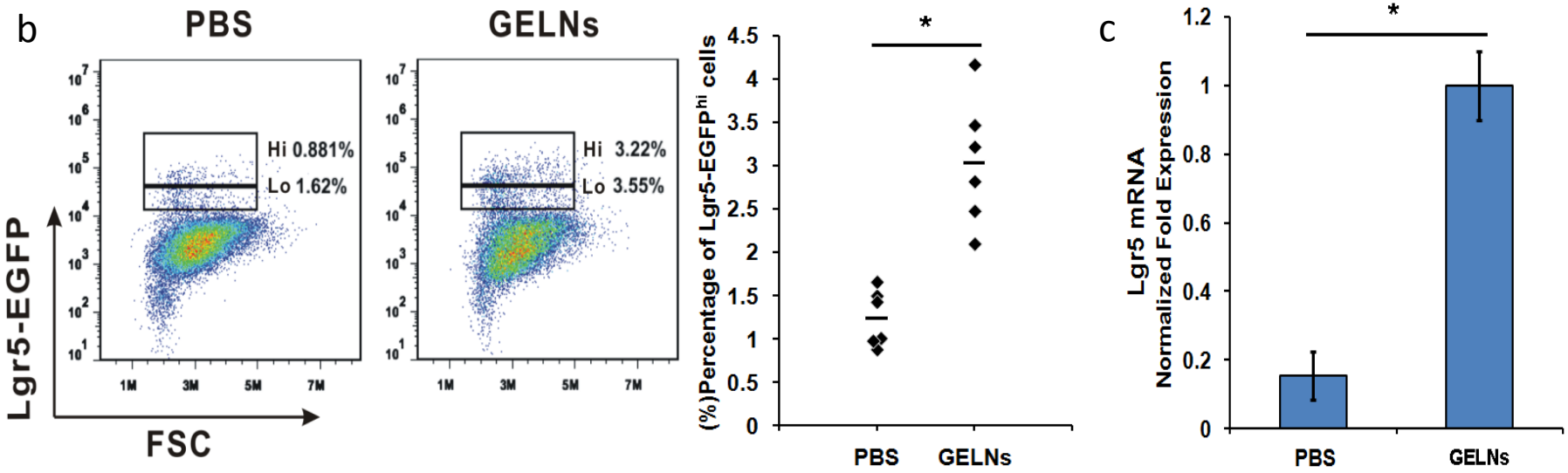
b
PBS
GELNs
Hi 0.881%
Lo 1.62%
Hi 3.22%
Lo 3.55%
Lgr5-EGFP
FSC
1M
3M
5M
7M
(%)Percentage of Lgr5-EGFP^hi cells
PBS
GELNs
*
c
Lgr5 mRNA
Normalized Fold Expression
PBS
GELNs
*

Figure 3

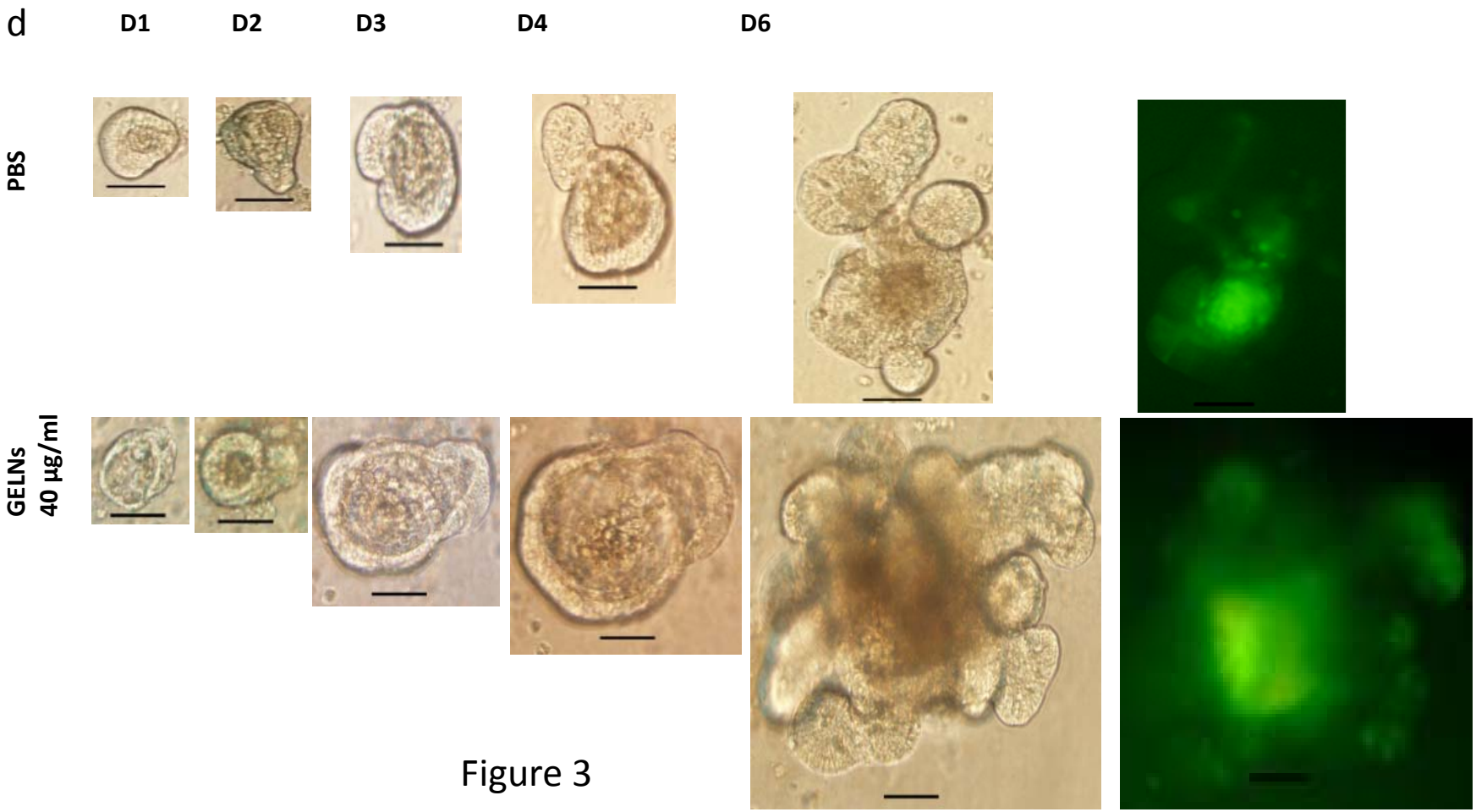


Figure 3

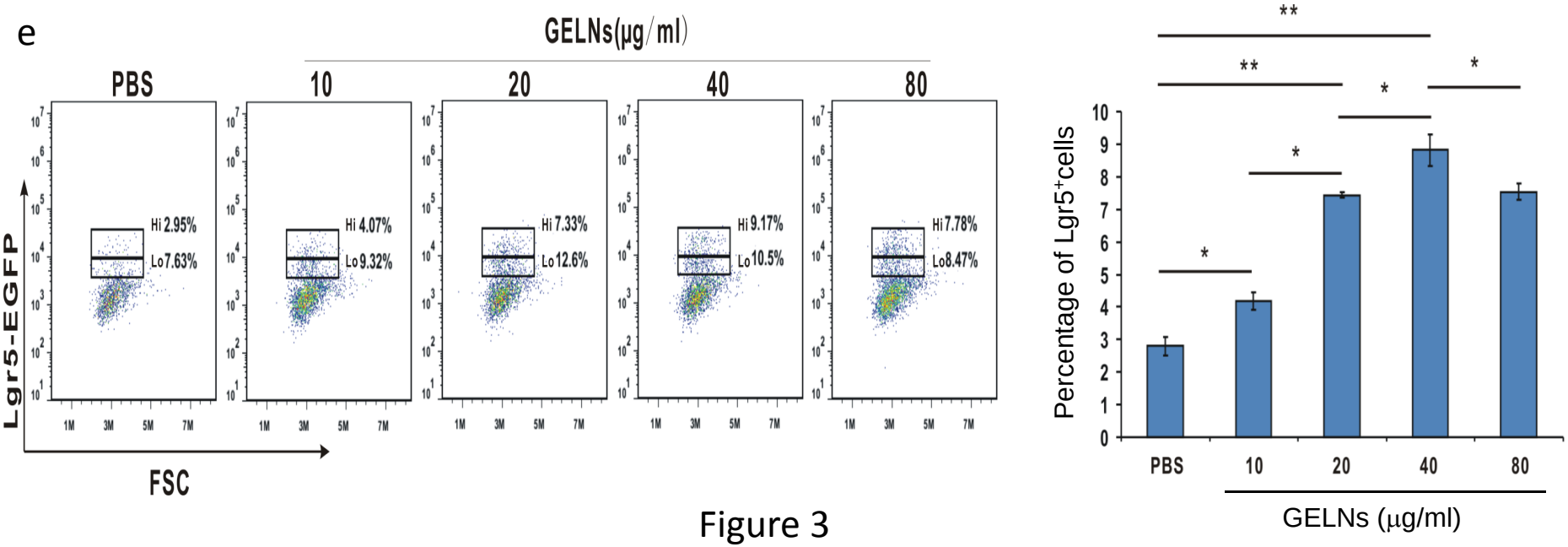
e
GELNs(μg/ml)
PBS
10
20
40
80
Hi 2.95%
Lo 7.63%
Hi 4.07%
Lo 9.32%
Hi 7.33%
Lo 12.6%
Hi 9.17%
Lo 10.5%
Hi 7.78%
Lo 8.47%
Lgr5-EGFP
FSC
1M
3M
5M
7M
Percentage of Lgr5+cells
PBS
10
20
40
80
GELNs (μg/ml)

Figure 3

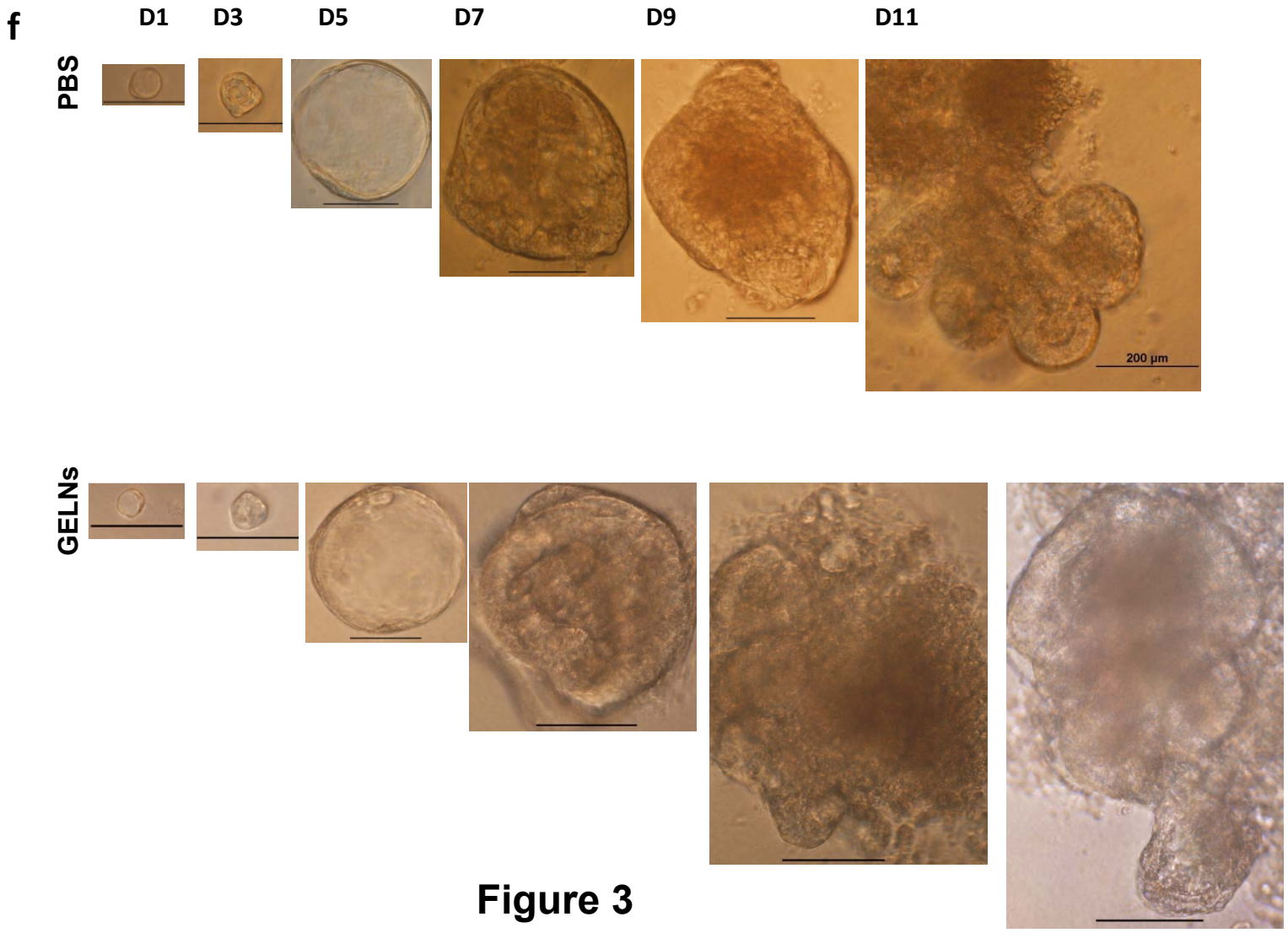


Figure 3

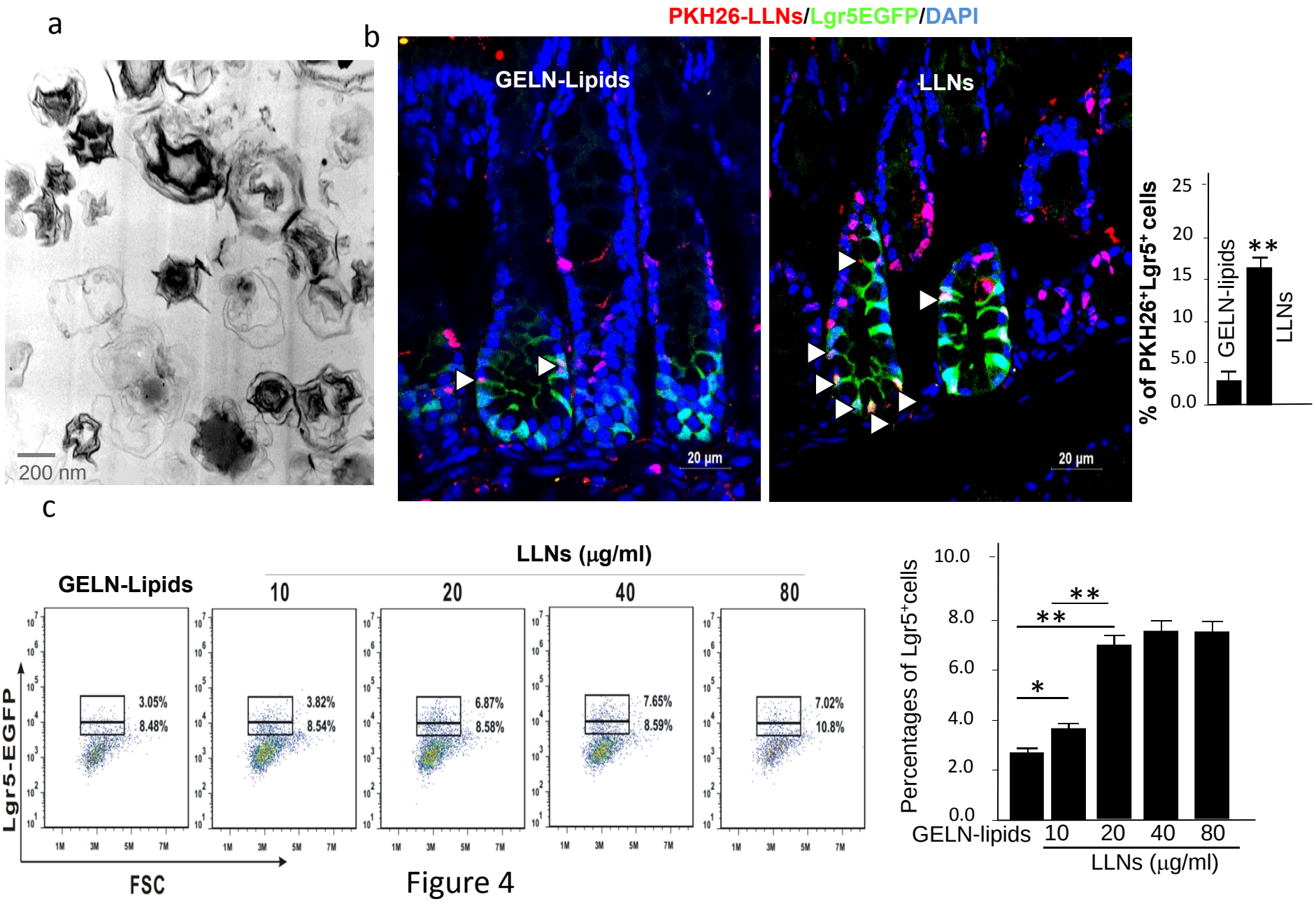
a
200 nm
b
PKH26-LLNs/Lgr5EGFP/DAPI
GELN-Lipids
LLNs
20 μm
20 μm
% of PKH26+Lgr5+ cells
25
20
15
10
5.0
0.0
GELN-lipids
LLNs
**
c
LLNs (μg/ml)
GELN-Lipids
10
20
40
80
Lgr5-EGFP
FSC
3.05%
8.48%
3.82%
8.54%
6.87%
8.58%
7.65%
8.59%
7.02%
10.8%
Percentages of Lgr5+cells
10.0
8.0
6.0
4.0
2.0
0.0
*
**
**
GELN-lipids
10
20
40
80
LLNs (μg/ml)

Figure 4

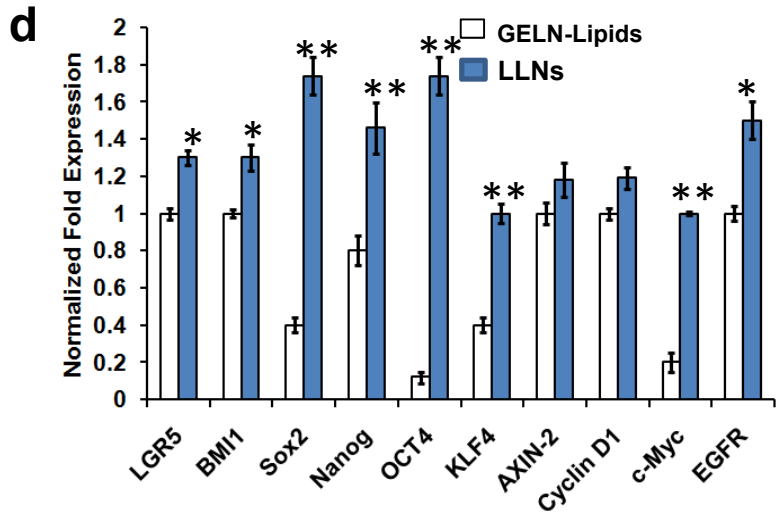
d
GELN-Lipids
LLNs
Normalized Fold Expression
2
1.8
1.6
1.4
1.2
1
0.8
0.6
0.4
0.2
0
LGR5
BMI1
Sox2
Nanog
OCT4
KLF4
AXIN-2
Cyclin D1
c-Myc
EGFR

Figure 4

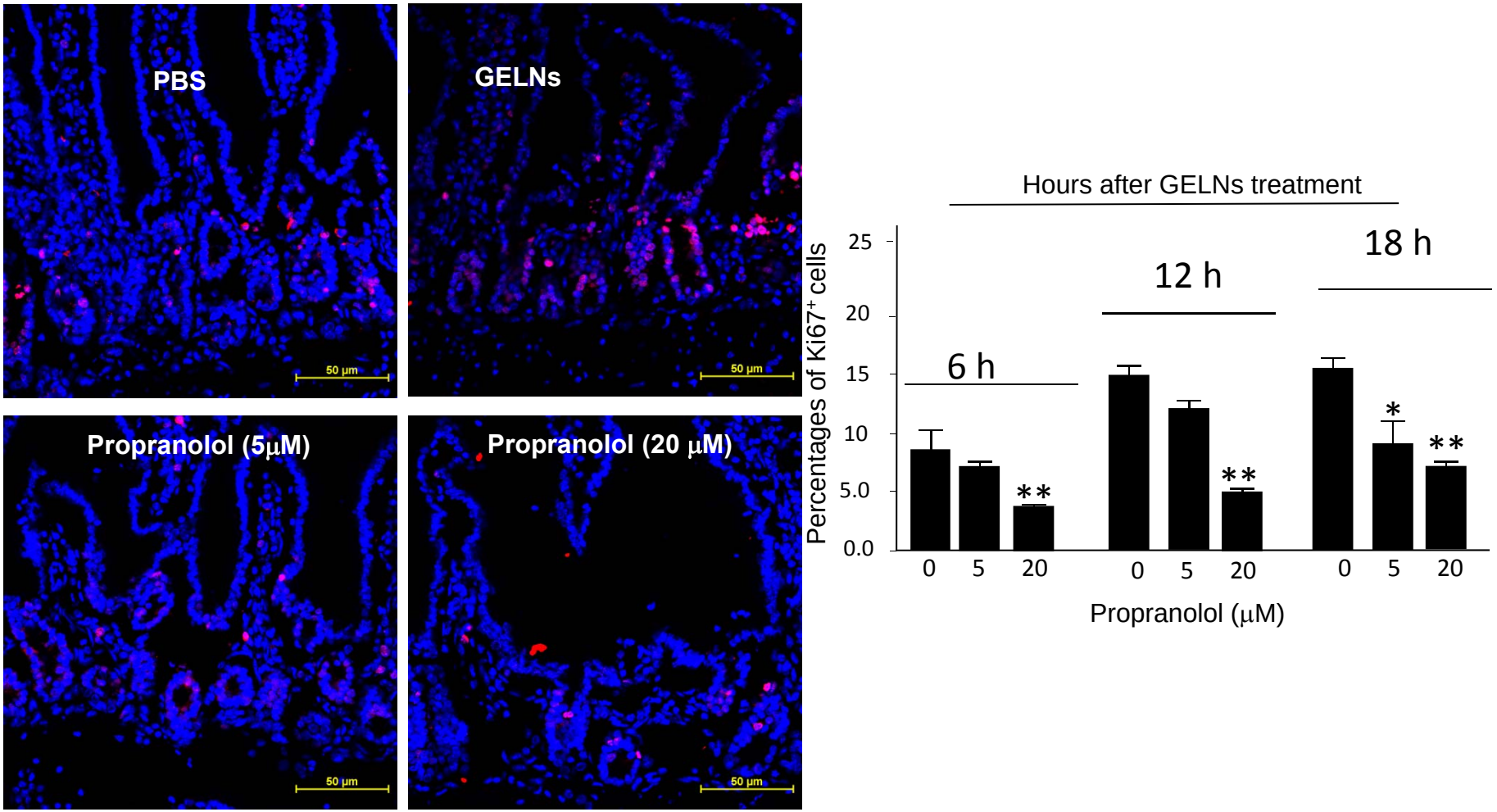
PBS
GELNs
Propranolol (5μM)
Propranolol (20 μM)
50 μm
Hours after GELNs treatment
6 h
12 h
18 h
Percentages of Ki67+ cells
25
20
15
10
5.0
0.0
0
5
20
Propranolol (μM)
*
**

Figure 4e

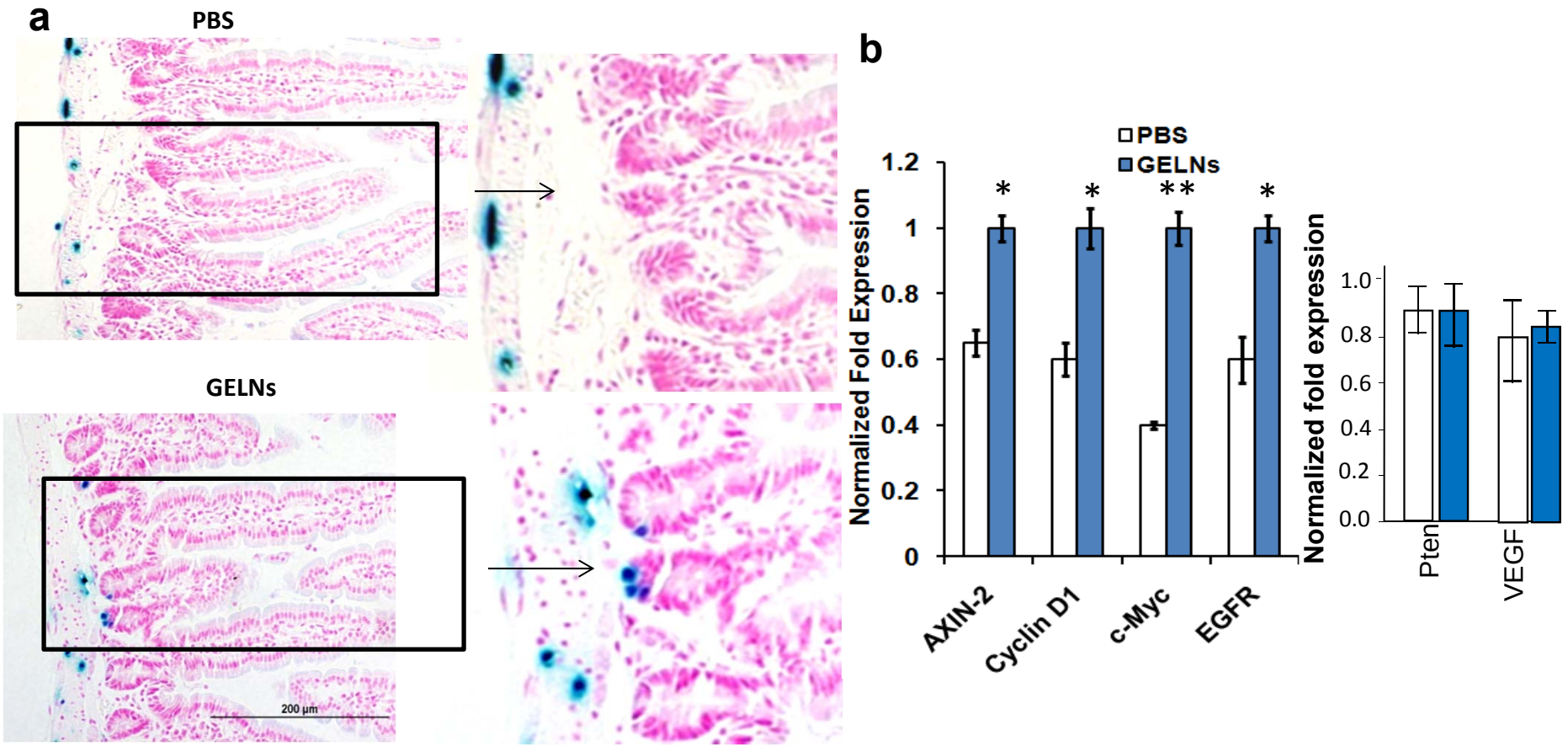
a
PBS
GELNs
200 μm
b
PBS
GELNs
Normalized Fold Expression
1.2
1
0.8
0.6
0.4
0.2
0
*
*
**
*
AXIN-2
Cyclin D1
c-Myc
EGFR
Normalized fold expression
1.0
0.8
0.6
0.4
0.2
0.0
Pten
VEGF

**Figure 5**

c

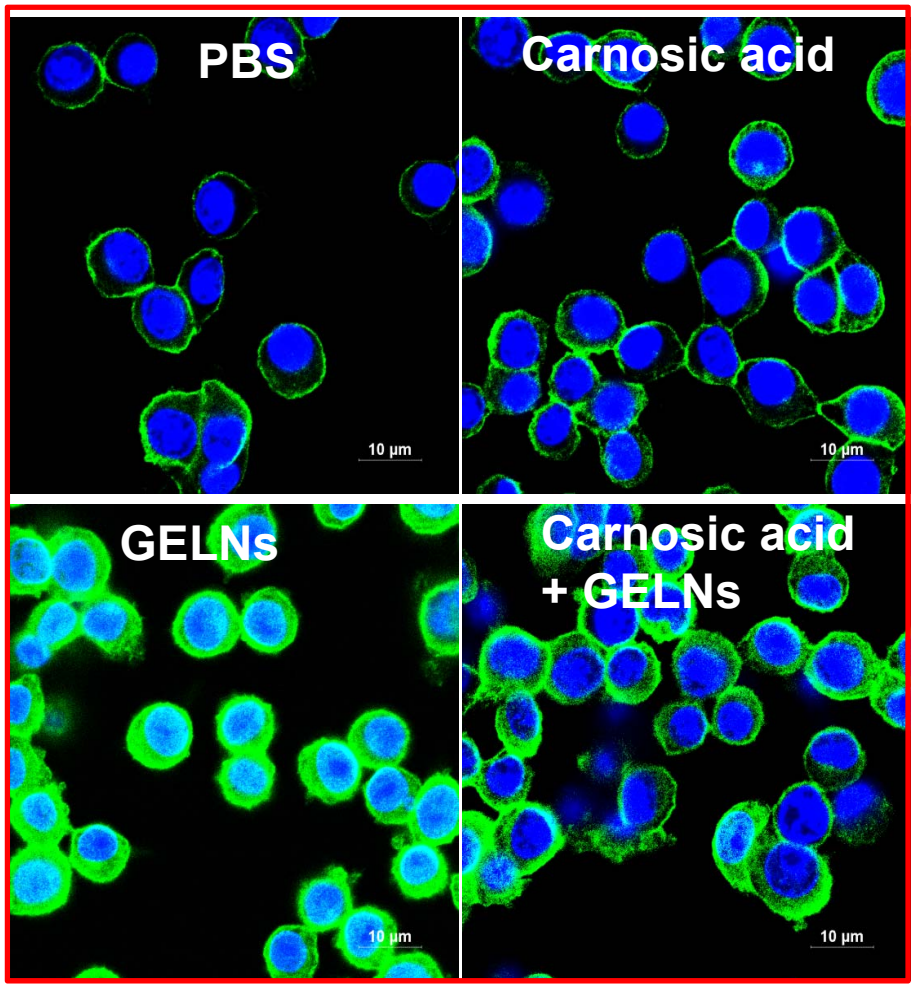
PBS
Carnosic acid
GELNs
Carnosic acid
+ GELNs
10 μm
10 μm
10 μm
10 μm

**Figure 5**

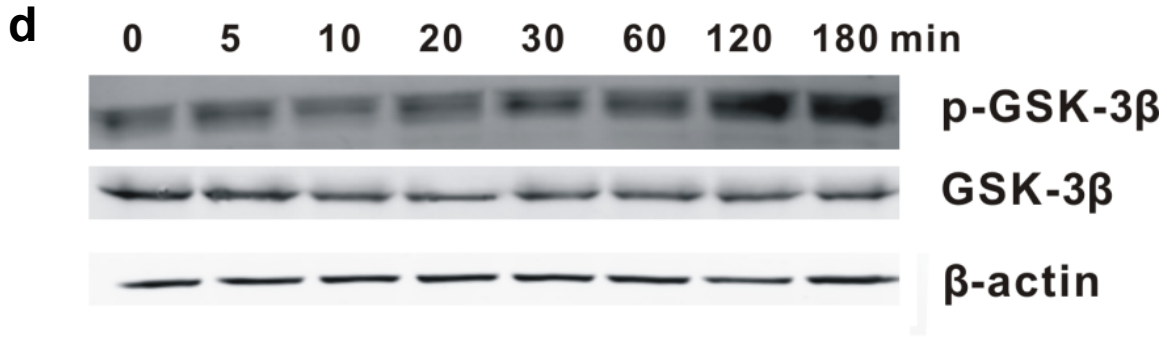
d
0
5
10
20
30
60
120
180 min
p-GSK-3β
GSK-3β
β-actin

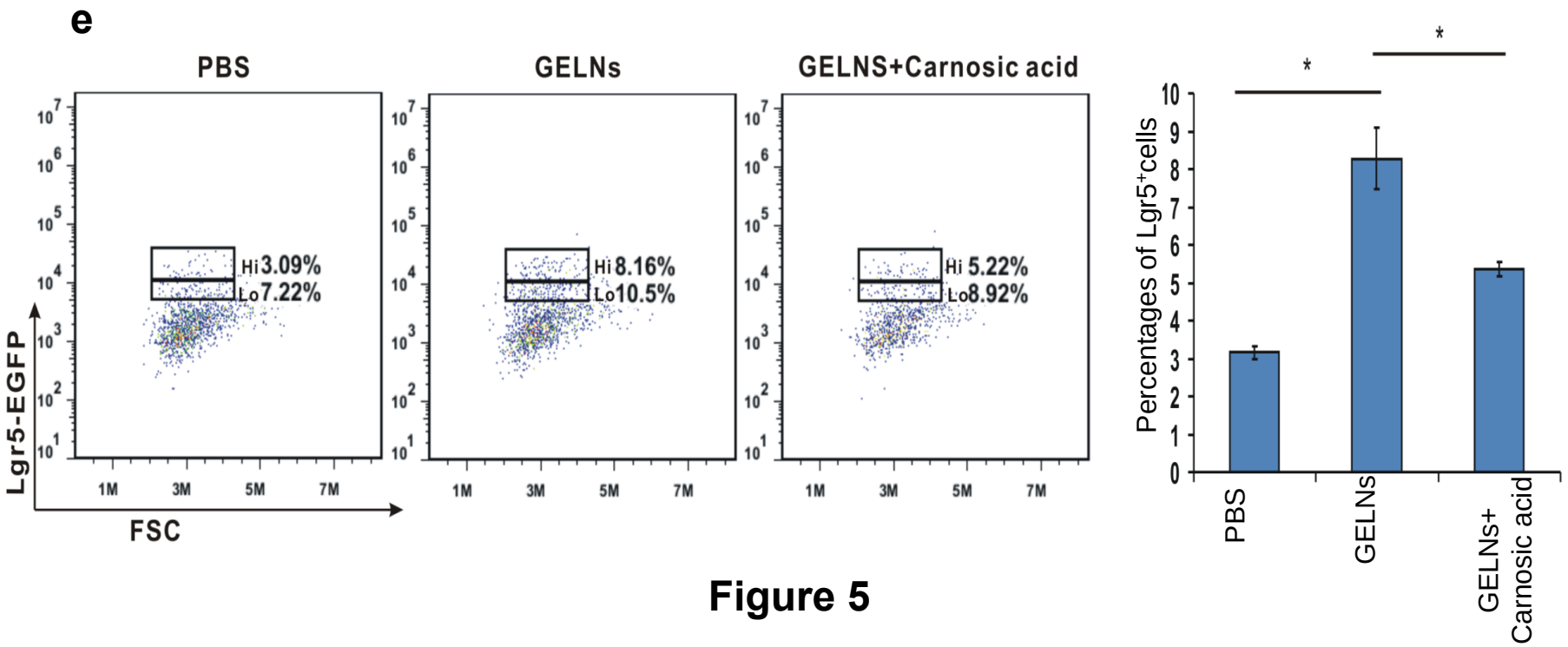
e
PBS
GELNs
GELNS+Carnosic acid
Hi 3.09%
Lo 7.22%
Hi 8.16%
Lo 10.5%
Hi 5.22%
Lo 8.92%
Lgr5-EGFP
FSC
1M
3M
5M
7M
Percentages of Lgr5+cells
PBS
GELNs
GELNs+ Carnosic acid
*
*

**Figure 5**

f

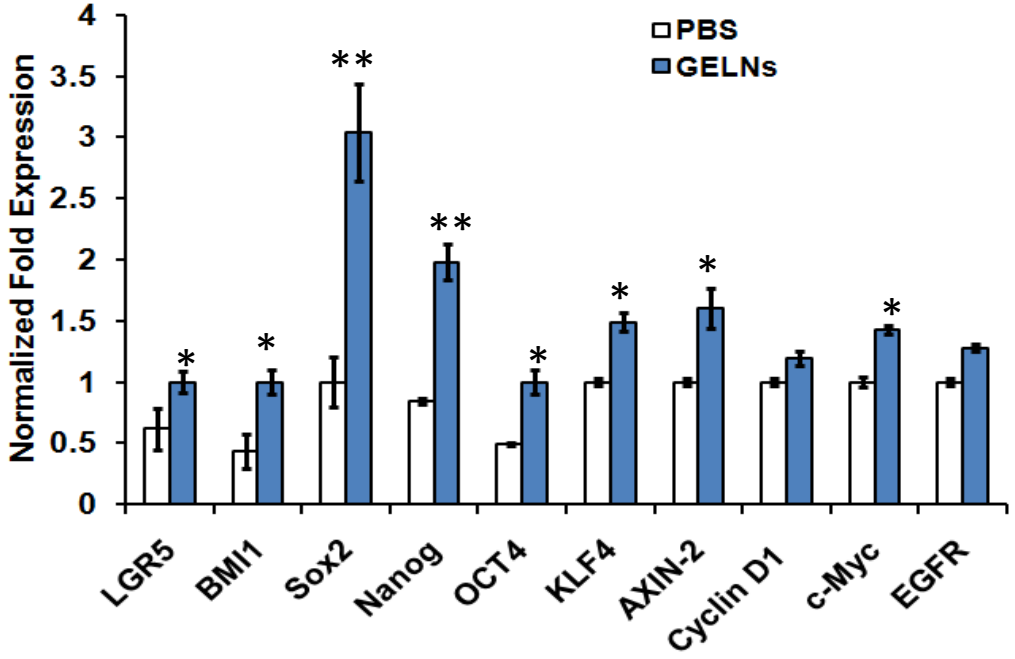
PBS
GELNs
Normalized Fold Expression
4
3.5
3
2.5
2
1.5
1
0.5
0
*
*
**
**
*
*
*
*
LGR5
BMI1
Sox2
Nanog
OCT4
KLF4
AXIN-2
Cyclin D1
c-Myc
EGFR

**Figure 5**

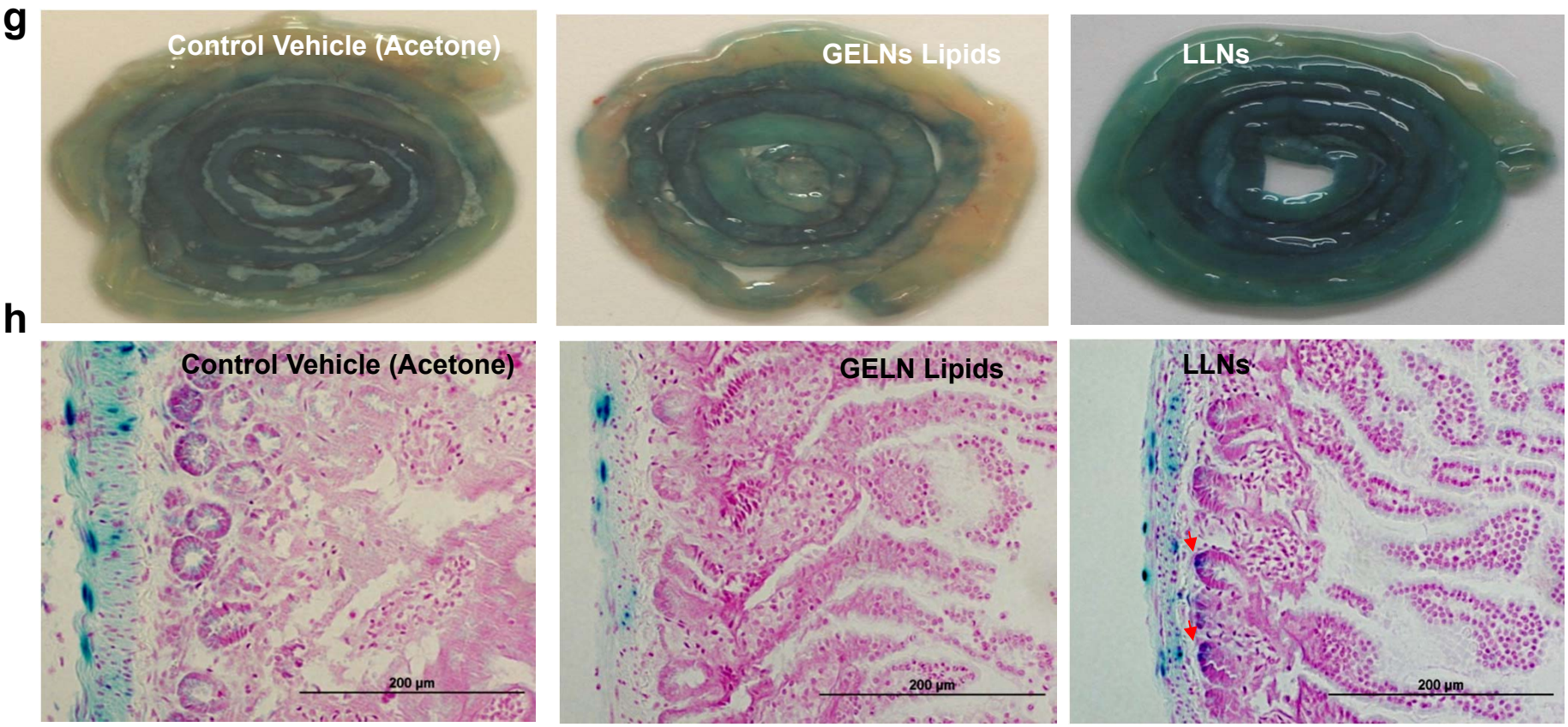
g
Control Vehicle (Acetone)
GELNs Lipids
LLNs
h
Control Vehicle (Acetone)
GELN Lipids
LLNs
200 µm
200 µm
200 µm

**Figure 5**

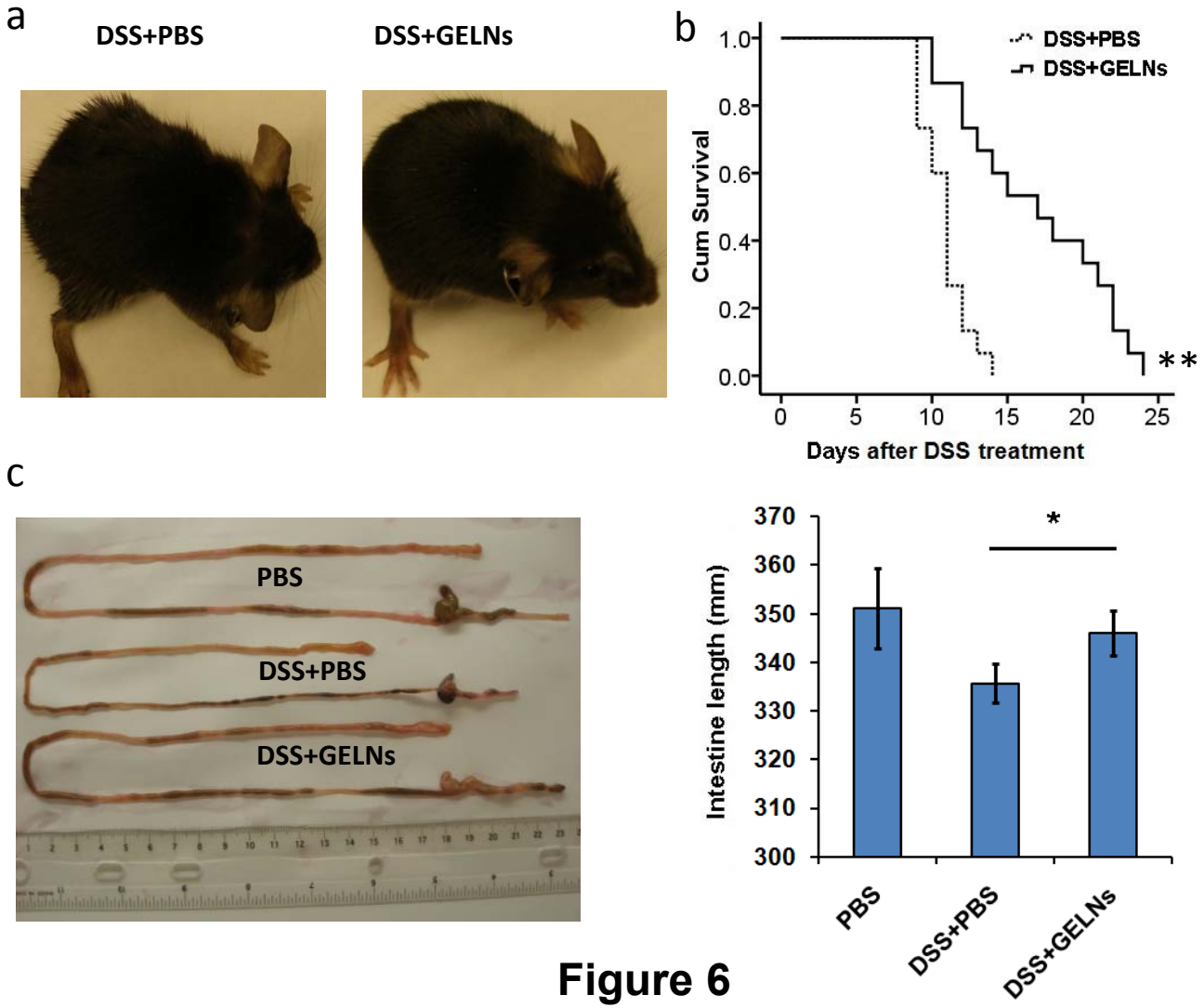
a
DSS+PBS
DSS+GELNs
b
DSS+PBS
DSS+GELNs
Cum Survival
1.0
0.8
0.6
0.4
0.2
0.0
0
5
10
15
20
25
Days after DSS treatment
**
c
PBS
DSS+PBS
DSS+GELNs
Intestine length (mm)
370
360
350
340
330
320
310
300
*
PBS
DSS+PBS
DSS+GELNs

**Figure 6**

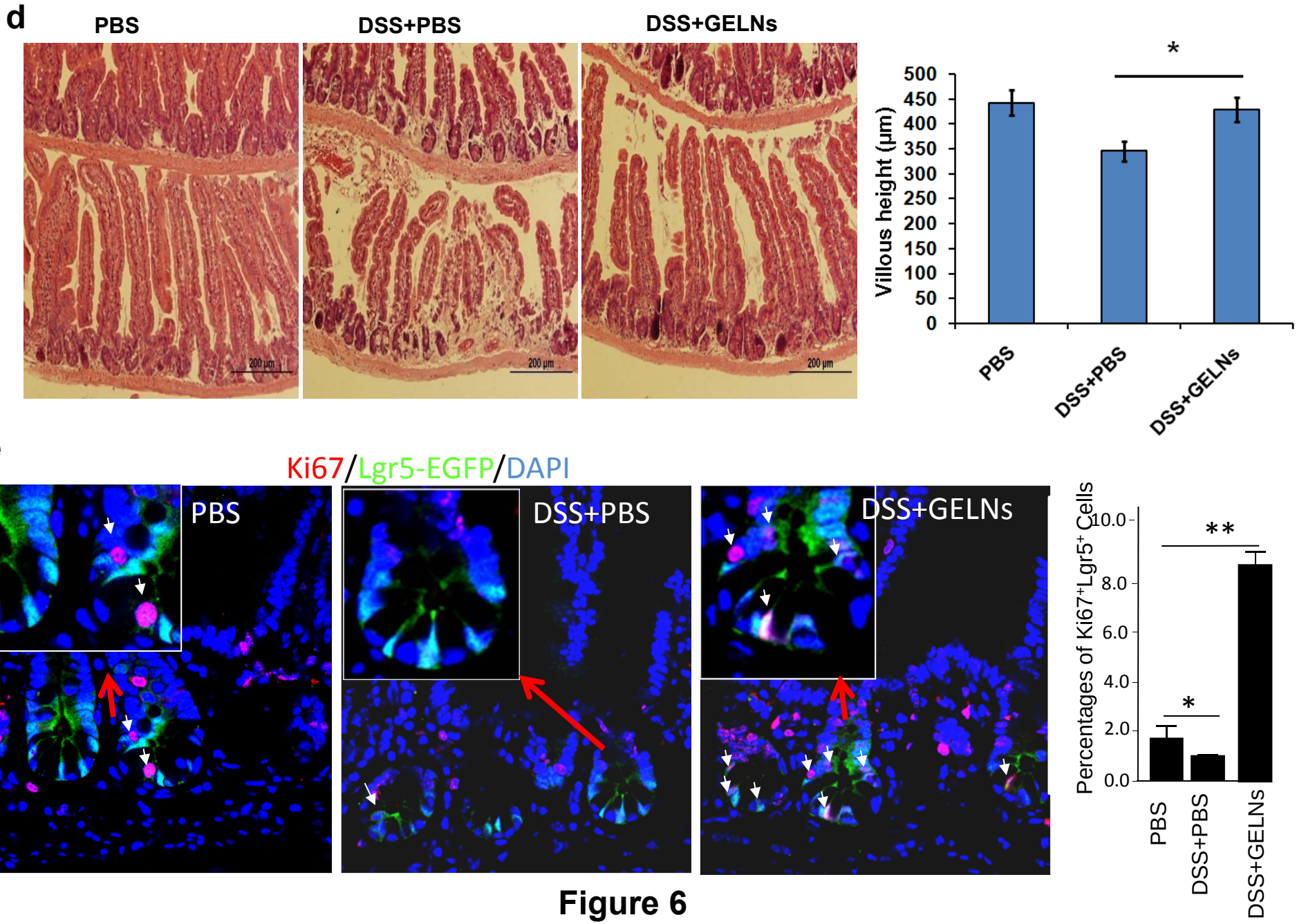
d
PBS
DSS+PBS
DSS+GELNs
200 μm
200 μm
200 μm
*
Villous height (μm)
500
450
400
350
300
250
200
150
100
50
0
PBS
DSS+PBS
DSS+GELNs
e
Ki67/Lgr5-EGFP/DAPI
PBS
DSS+PBS
DSS+GELNs
Percentages of Ki67+Lgr5+ Cells
10.0
8.0
6.0
4.0
2.0
0.0
**
*
PBS
DSS+PBS
DSS+GELNs

**Figure 6**

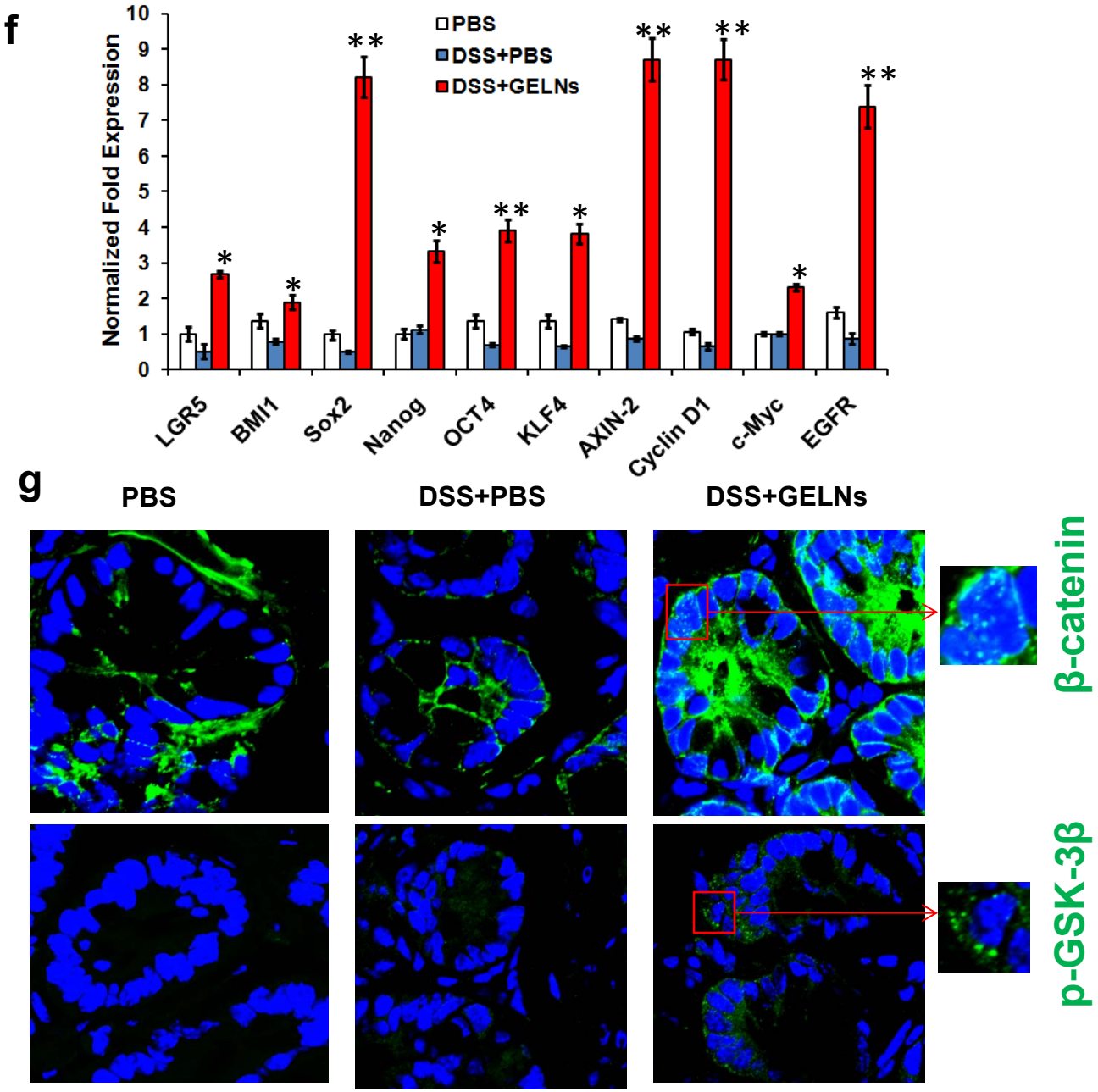
f
Normalized Fold Expression
PBS
DSS+PBS
DSS+GELNs
LGR5
BMI1
Sox2
Nanog
OCT4
KLF4
AXIN-2
Cyclin D1
c-Myc
EGFR
g
PBS
DSS+PBS
DSS+GELNs
β-catenin
p-GSK-3β

Figure 6

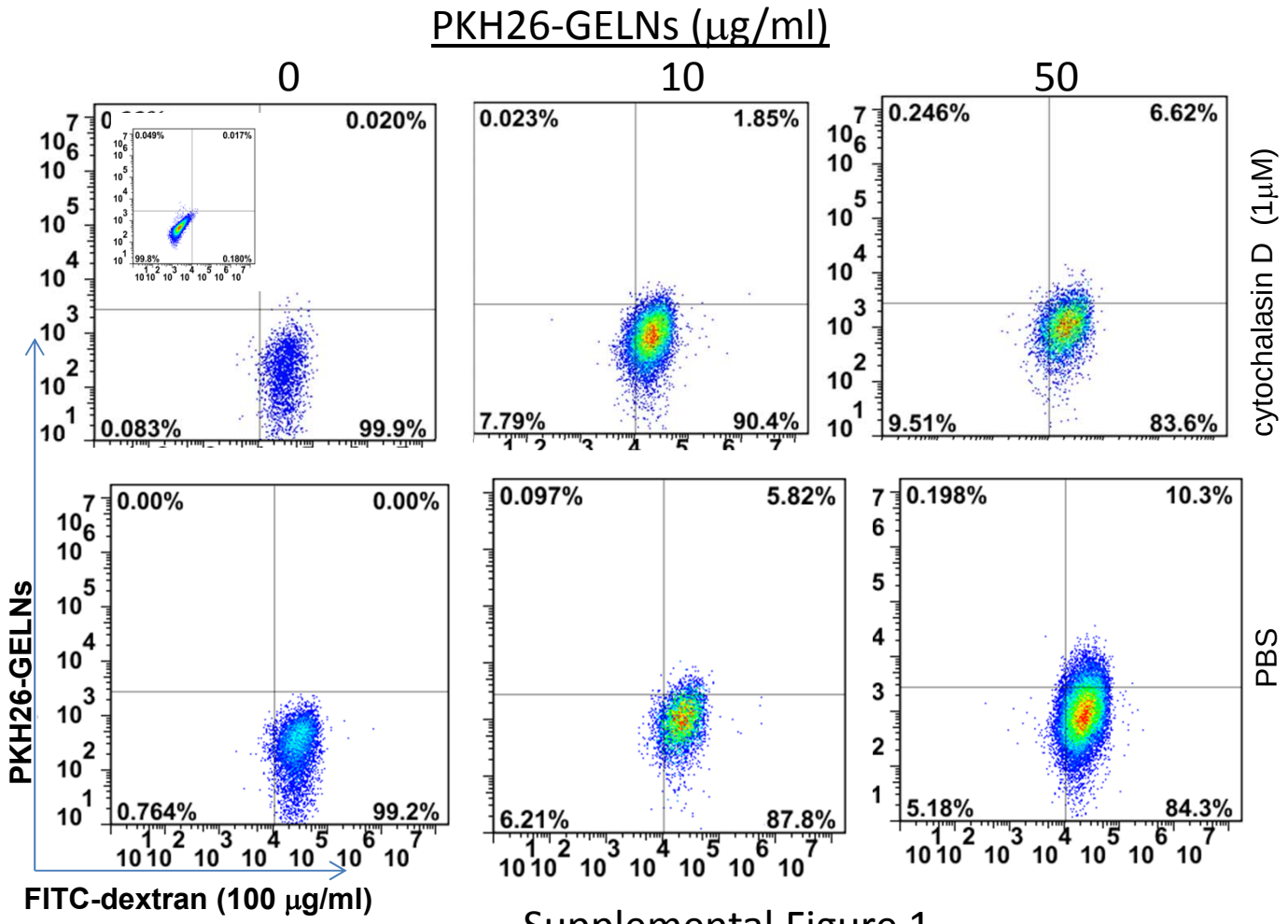


Supplemental Figure 1

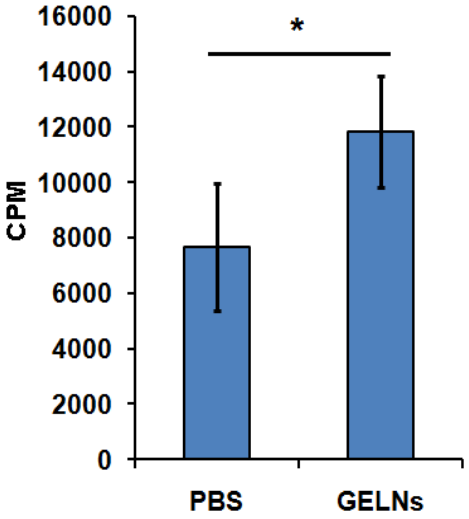


Supplemental figure 2

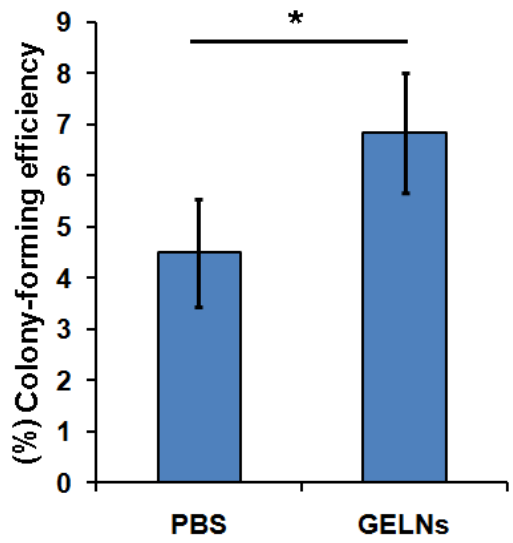


Supplemental figure 3

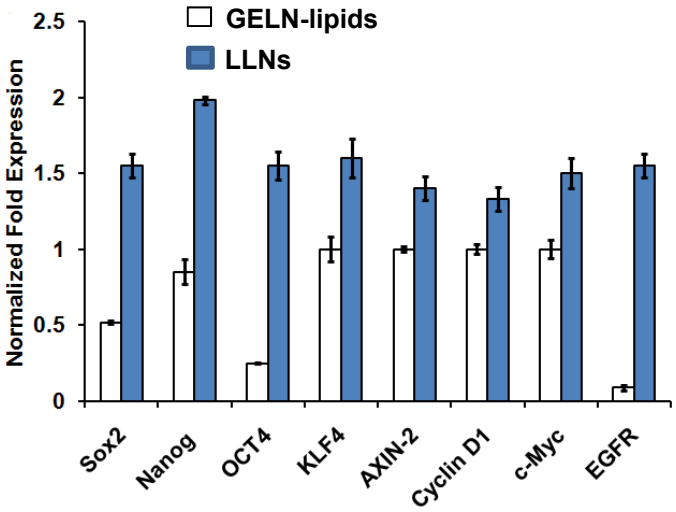


Supplemental figure 4

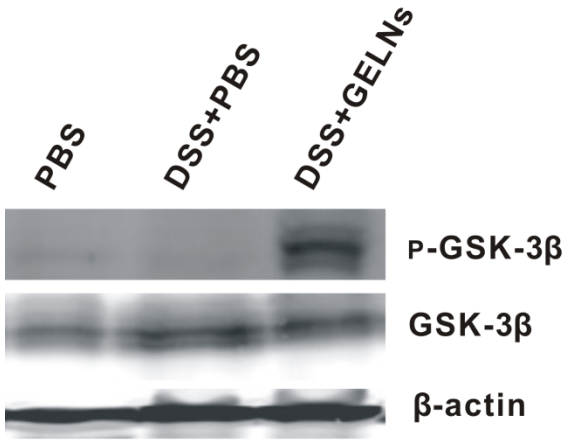


Supplemental figure 5

## Supplemental Material and Methods

### Mice

C57BL/6j mice, Lgr5-EGFP-ires-creERT2 mice, and TCF/LEF-reporter mice (B6.Cg-Tg (BAT-lacZ)3Picc/J) 6-12 weeks of age were obtained from Jackson Laboratories. All animal procedures were approved by the University of Louisville Institutional Animal Care and Use Committee. Mice were administered by gavage grape exosome-like nanoparticles resuspended in PBS as described previously[1].

### In vivo image of gavaged GELNs

Mice were first anesthetized with ketamine (100 mg/kg body weight) and xylazine (10 mg/kg body weight) via intraperitoneal injection: inhaled isoflurane was used as necessary. To monitor the trafficking of GELNs administered via oral gavage, GELNs (1mg/mouse) were first labeled with a near-infrared lipophilic carbocyanine dye-dioctadecyl-tetramethylindotricarbocyanine iodide (DIR, Invitrogen, Carlsbad, CA) using a previously described method[2]. The mice were imaged over a 48-hour period using a Carestream Molecular Imaging system (Carestream Health, Woodbridge, CT). For controls, mice (five per group) received free DIR dye in PBS at the same concentration for DIR dye-labeled GELNs. Images were collected using a high-sensitivity CCD camera with an exposure time of 2 minutes for imaging.

To determine whether $Lgr5^+$ intestinal stem cells take up GELNs, Lgr5-EGFP-IRES-CreERT2 mice starved overnight were given 1 mg PKH26 (Sigma) fluorescent dye labeled GELNs/mouse by gavage in 100 μl of PBS. 6 h after gavaging, mice were

sacrificed and intestinal tissues were embedded in OCT compound (Miles Laboratories; Elkhart, IN) and frozen. Tissues were sectioned 5 μm thick with a cryostat and mounted on commercially provided charged slides (Fisher Scientific; Pittsburgh, PA) for immunohistological and DAPI (Molecular Probe) staining. Images were acquired with a Zeiss LSM 510 confocal microscope equipped with a digital image analysis system (Pixera).

**Immunohistochemical staining**

For histopathology, H&E staining was performed on paraffin-embedded intestinal sections. For immunofluorescence analysis, OCT (Sakura Finetek)-embedded tissue cryosections (9μm-thick) were fixed at -20°C in methanol/acetone (3:1). Slides were hydrated in PBS and blocked for 30 min at 25°C with Fc Block (10 μg/ml) and 5% (vol/vol) normal horse serum in PBS. After blocking, slides were incubated for 30 min at 25°C with the following primary antibodies in PBS: anti-β-catenin, anti-pGSK-3β (Cell signaling), anti-EPCAM (BD Biosciences), anti-ki67 (Thermo Scientific), and anti-lysosome (R&D Systems). Primary antibodies were detected with a secondary antibody to fluorescein isothiocyanate–Alexa Fluor 488 (Invitrogen). Slides were mounted with Slow Fade Gold Antifade plus DAPI (4,6-diamidino-2-phenylindole; S36938; Molecular Probes). Stained slides were assessed using a Zeiss LSM 510 confocal microscope equipped with a digital image analysis system (Pixera).

**LacZ staining**

To assess the treatment effects on expression of lacZ gene regulation by Tcf4 promoter, B6.Cg-Tg ((BAT-lacZ)3Picc/J) mice were gavage administered carnosic acid (Sigma-Aldrich) (7.5mg/kg/day), GELNs, or carnosic acid encapsulated GELNs at an equal amount to carnosic acid alone (7.5mg/kg/day) or PBS as a control vehicle for 5 days. Mice were sacrificed and small intestinal tissue segments were fixed in 0.2% glutaraldehyde, 50 mM EGTA, pH 7.3, 100 mM $MgCl_2$ in PBS. Staining was performed overnight in staining buffer (0.5 mg/ml X-gal, 5 mM potassium ferrocyanide, 5 mM potassium ferricyanide in 2 mM $MgCl_2$, 0.01% sodium deoxycholate, 0.02% Nonidet P40 in PBS; pH 7.3). The next day, intestinal segments were washed in PBS, counterstained with nuclear fast red, and covered in Kaiser's glycerogelatin. All pictures were taken with an IX71 inverted microscope (Olympus). Swiss-rolled small intestines of ((BAT-lacZ)3Picc/J) mice were also fixed and stained with X-gal and examined in a blinded manner by a gastrointestinal pathologist.

**Western Blot Analysis.** Western blots were carried out as described previously [1]. In brief, cells or homogenized intestinal tissues were lysed in radioimmunoprecipitation assay lysis buffer (1% Triton X-100, 0.1% SDS, 150 mM NaCl, 50 mM Tris-HCl, 1 mM EDTA, 1 mM EGTA, 5 mM sodium molybdate, and 20 mM phenylphosphate) with protease and phosphatase inhibitors (1 mM PMSF, 10 µg/ml aprotinin, 20 µg/ml leupeptin, 20 µg/ml pepstatin A, 50 mM NaF, and 1 mM sodium or thovanadate). Proteins of lysed cells were separated by SDS-PAGE on 10% polyacrylamide gels. The membranes were stained with Ponceau Red to validate that all samples contained similar amounts of protein. Separated proteins were transferred to nitrocellulose

membranes for western blotting using a standard protocol as described previously[3]. The following antibodies were purchased from Cell Signaling Technology Inc. and used for western blot analysis: Rabbit polyclonal anti–β-catenin, anti–phospho β-catenin (S675), anti-phosphor GSK3 (Ser9), anti-GSK3, and anti-Wnt5a. Polyclonal anti-A33 antibody was purchased from Santa Cruz Biotechnology.

**RNA extraction and real-time PCR.** Total RNA was isolated from intestinal crypts or the CT26 cell line with TRIzol according to the manufacturer's specifications (Invitrogen) and was repurified with an RNeasy mini kit (Qiagen). RNA (1µg) was reverse-transcribed with Superscript III and random primers (Invitrogen). For quantitation of genes of interested, cDNA samples were amplified in a CFX96 Realtime System (Bio-Rad Laboratories, Hercules, CA, USA) and Sso Fasteva green supermixture (Bio-Rad Laboratories) according to the manufacturer's instructions. Fold changes in mRNA expression between treatments and controls were determined by the δCT method as described[4]. Differences between groups were determined using a two-sided Student's *t*-test and one-way ANOVA. Error bars on plots represent ± SE, unless otherwise noted. The data were normalized to a GAPDH reference. All primers were purchased from Eurofins MWG Operon. The primer pairs for analysis are provided in Supplementary Table 4. All assays were performed in triplicate at least three times.

**Proteomic Analysis.** GELNs were lysed in protein lysis buffer and 100 µg of proteins were electrophoresed on 10% SDS-polyacrylamide gels. Coomassie-stained SDS-polyacrylamide gels were cut into 10 strips to correlate with the gel lanes and

trypsinized. The digested peptides were loaded on a 100 nm × 10 cm capillary column packed in-house with C18 Monitor 100 A-spherical silica beads and eluted by a 1 h gradient of 10–100% acetonitrile, 0.1% TFA. Mass spectrometry analysis was performed and analyzed using an LTQ XL spectrometer (Thermo Finnigan) at the UAB Proteomic Core Facility. Protein hits were validated using a method as described[5].

**GELN miRNA microarray analysis**

Total RNA containing miRNA was extracted from GELNs using the SNC50-kit (Sigma). One hundred nanograms of small RNA enriched samples were submitted to Phalanx Biotech Group, Inc. (Belmont, CA 94002 USA) for miRNA microarray analysis.

**Internalisation assay**

CT26 cells were cultured for 12 hours in the growth medium. Uptake of GELNs was performed by incubating 12 h cultured CT26 cells with various dilutions of PKH26 fluorescent dye labeled GELNs (PKH26-GELNs) in a humid chamber for 2 hours (37°C, 5% $CO_2$). For inhibition experiments, cell cultures were pre-incubated with the inhibitors for 30 minutes before PKH26-GELNs were added to the culture. The percentage of up taking of PKH26-GELNs was FACS analyzed using a method as described [6].

The following inhibitors were used: bafilomycin A1, concanamycin A, chlorpromazine, indomethacin, and cytochalasin D from *Zygosporium manonsii*. The inhibitors were purchased from Sigma and FITC-dextran 40 kDa (Molecular Probes).

Additionally, for the macropinocytosis assay, CT26 cells were given FITC-dextran (100 μg/ml) or FITC-dextran plus PKH26-GELNs in PBS, 2% FCS for 30 min at 4°C to block endocytosis, and then the temperature was shifted to 37°C for 3 h in the presence of cytochalasin D (1 μM). CT26 cells were then washed and analyzed using a flow cytometer.

**Intestinal organ culture**. The clean mucosal layer of Lgr5-EGFP-ires-creERT2 mice was washed in Hank's Balanced Salt Solution buffer and cut with a sterile scalpel into 2 $cm^2$ pieces. The pieces were placed on sterile metal grids and cultured in Dulbecco's Modified Eagle Medium supplemented with 10% exosome-depleted fetal bovine serum, epidermal growth factor (200 ng/ml, Peprotech) and Insulin-Transferrin-Selenium-X (10 μl/ml, Invitrogen). For the internalization assay, PKH26-GELNs were added to the culture at the beginning of culture in the present or absent of cytochalasin D for 6 h. Then, the treated tissue was fixed for quantification of PKH26-GELNs$^+$Lgr5$^+$ cells. Propranolol is known to induce rapid activation of PLD activity. For determination of the possible effect of propranolol mediated PA activity on LLN induced intestinal epithelium proliferation, colon tissue was cultured with propranolol (5μM) for 1 h prior to addition of LLNs (20 μg/ml). 12 h cultured colon tissue was then frozen sectioned and stained with anti-Ki67 antibody and examined in a blinded manner. 10 viewing field images of each sample were randomly captured.

References

1. Sun, D*, et al.* (2010). A novel nanoparticle drug delivery system: the anti-inflammatory activity of curcumin is enhanced when encapsulated in exosomes. *Mol Ther* **18**: 1606-1614.
2. Zhuang, X*, et al.* (2011). Treatment of brain inflammatory diseases by delivering exosome encapsulated anti-inflammatory drugs from the nasal region to the brain. *Mol Ther* **19**: 1769-1779.
3. Liu, Y*, et al.* (2009). COP9-associated CSN5 regulates exosomal protein deubiquitination and sorting. *Am J Pathol* **174**: 1415-1425.
4. Xiang, X*, et al.* (2011). miR-155 promotes macroscopic tumor formation yet inhibits tumor dissemination from mammary fat pads to the lung by preventing EMT. *Oncogene* **30**: 3440-3453.
5. Xiang, X*, et al.* (2009). Induction of myeloid-derived suppressor cells by tumor exosomes. *Int J Cancer* **124**: 2621-2633.
6. Deng, Z*, et al.* (2012). Tumor cell cross talk with tumor-associated leukocytes leads to induction of tumor exosomal fibronectin and promotes tumor progression. *Am J Pathol* **180**: 390-398.

**Supplemental Figure legends:**

**Supplemetnal Figure 1 GELNs taken up by intestinal epithelial cells.** Mouse CT26 intestinal epithelial cells were incubated with 100 µg/ml high molecular weight dextran for 30 min "on ice", followed by a 37°C incubation for 30 min. Cells were then treated with PKH26-GELNs at variable doses and incubated at 37°C for 3h. The percentage of FITC-dextran PKH26-GELN$^{+}$ CT26 cells was FACS determined. Unstained CT26 cells were used as a control (inset, top left corner). One representative result of three independent experiments is shown.

**Supplemetnal Figure 2.** Proliferation of cultured crypt cells stimulated by GELNs (40µg/ml) were measured by a $^{3}$H-thymidine incorporation assay. The results represent the mean ± SEM of five independent experiments (n=5).

**Supplemetnal Figure 3.** Colony-forming efficiency was calculated from 100 single sorted Lgr5-EGFP$^{hi}$ cells. The results represent the mean ± SEM of four independent experiments (n=4).

**Supplemetnal Figure 4.** Real-time analysis of the expression of different genes induced by nanoparticles assembled with GELN-lipids (40 μg/ml) in the CT26 colon cancer cell line at 12h after the treatments. Error bars represent the mean ± SEM of duplicate experiments (n=5).

**Supplemetnal Figure 5.** Western blotting analysis of phosphorylation of GSK-3β (Ser 9) and total GSK-3β 9) and β–actin from DSS treated C57BL/6 mice. One representative of three independent experiments is shown.

.

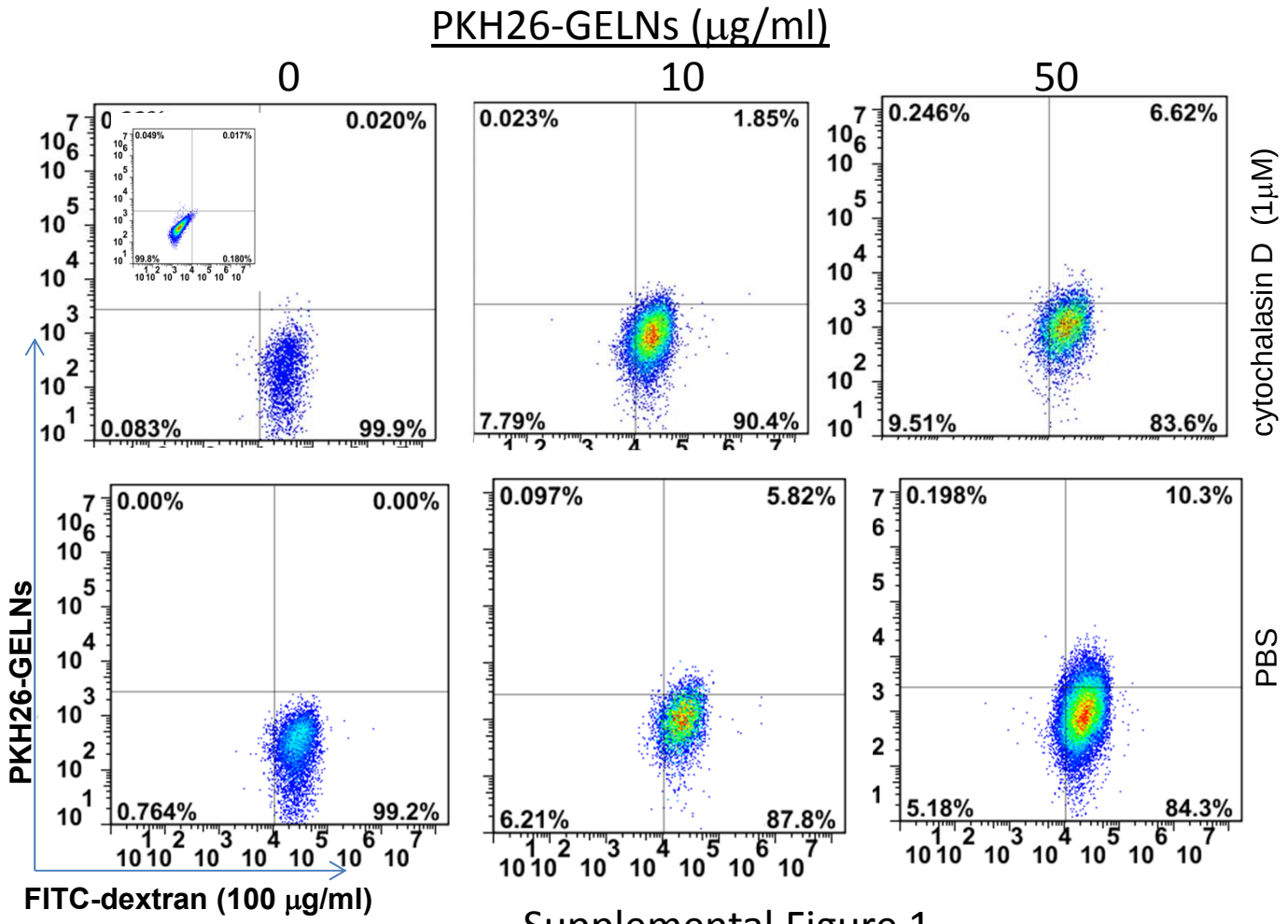


Supplemental Figure 1

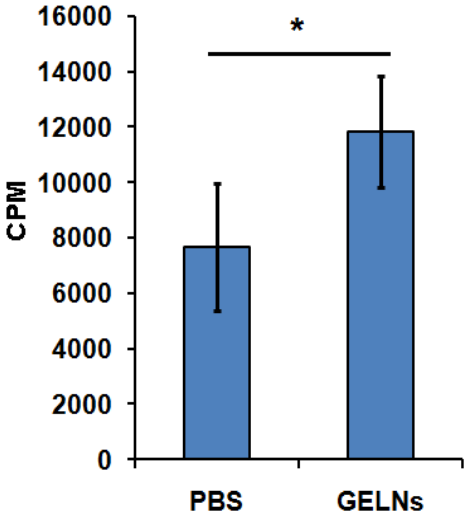


Supplemental figure 2

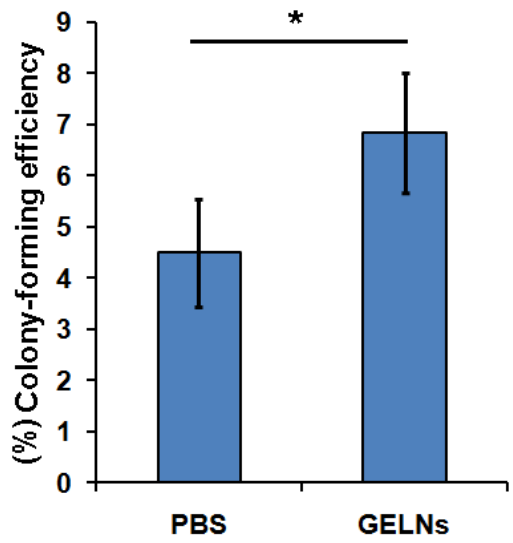


Supplemental figure 3

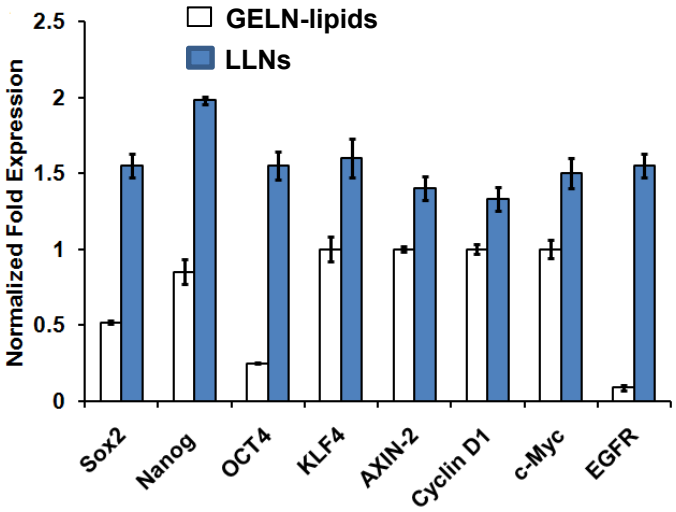


Supplemental figure 4

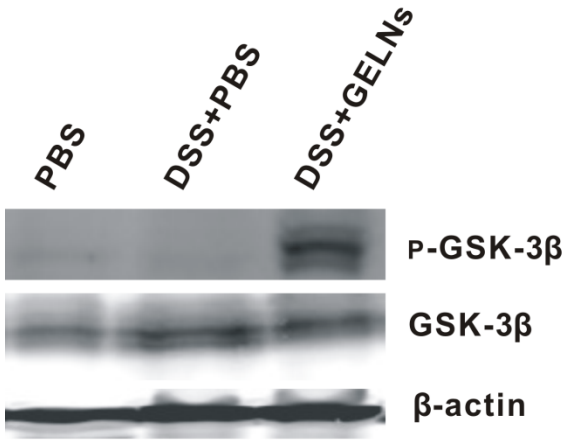


Supplemental figure 5